

**Validation of the Repurposing of the Niclosamide Scaffold for
the Design of PTEN-induced Putative Kinase 1 Modulators
with Potential Agonist Activity**

Submitted in partial fulfilment

of the requirements

of the Degree of Master of Pharmacy.

Abigail Buttigieg

Department of Pharmacy

2021



L-Università
ta' Malta

University of Malta Library – Electronic Thesis & Dissertations (ETD) Repository

The copyright of this thesis/dissertation belongs to the author. The author's rights in respect of this work are as defined by the Copyright Act (Chapter 415) of the Laws of Malta or as modified by any successive legislation.

Users may access this full-text thesis/dissertation and can make use of the information contained in accordance with the Copyright Act provided that the author must be properly acknowledged. Further distribution or reproduction in any format is prohibited without the prior permission of the copyright holder.

Dedicated to my brother Hayden, and my parents

Mary Rose and Emanuel for always supporting me.

Abstract

A mutation in the PTEN-induced putative kinase 1 (PINK 1) receptor has been shown to drive early onset Parkinson's disease. Evidence suggests that the anthelmintic drug niclosamide, shown to have good oral bioavailability and low toxicity, and other molecules bearing its basic scaffold are capable of activating PINK 1 through reversible mitochondrial membrane potential impairment resulting in a slower disease development. Thus PINK 1 is a target for the design of novel anti-parkinsonian drugs. This project aims to use the niclosamide scaffold as a lead molecule for the *in silico* identification and design of high affinity PINK 1 modulators, through virtual screening and *de novo* approach.

The PDB crystallographic deposition 5YJ9 describing the PINK1:ANP small molecule inhibitor complex was used in this study. The small molecule ANP601 was extracted from the ligand binding pocket (LBP) and molecular modelling of niclosamide was carried out. Niclosamide was docked into the LBP and conformational analysis was carried out to determine the best orientation which niclosamide can occupy within the LBP.

A consensus pharmacophore was created by superimposing the bioactive molecule ANP601 and the optimal niclosamide conformer, which was used to guide virtual screening and used as a query structure to identify analogous molecules. The rule of three was used as acceptance criteria on the identified hit structures, which were then filtered to ensure that all molecules were Lipinski rule compliant. The filtered molecules were docked in a protomol and ranked in order of affinity.

A map of the critical interactions between the optimal niclosamide conformer and the PINK1 LBP was used to guide the *de novo* approach. Seeds were generated by removing any inactive or unfavourable bonds from the optimal niclosamide conformer. The seed structures were docked in the LBP and allowed to grow. The resulting hits were filtered to ensure Lipinski rule compliance and ranked in order of affinity.

The molecules identified with the highest affinity towards the PINK1 LBP from both approaches are suggested for further optimisation.

Acknowledgments

I would like to express my sincere thanks to Dr. Claire Shoemake for her guidance and support throughout this project.

I would also like to extend my gratitude to the Head of Department, Professor Lillian M. Azzopardi, Professor Anthony Serracino Inglott and all the staff in the Pharmacy Department for their contribution to my education over these past five years.

Table of Contents

1. Introduction.....	2
1.1 Current Treatments for Parkinson’s Disease.....	2
1.1 PTEN-induced Putative Kinase 1 Receptor.....	3
1.2.1 Endogenous Agonists of PTEN-induced Putative Kinase 1.....	5
1.2.2 The Structure of PTEN-induced Putative Kinase 1.....	9
1.2.3 The Requirements of Binding to PTEN-induced Putative Kinase 1.....	11
1.2.4 Antagonists of PTEN-induced Putative Kinase 1.....	12
1.3 Niclosamide as a PTEN-induced Putative Kinase 1 Agonist.....	12
1.3.2 Literature on Niclosamide.....	12
1.3.2 Interactions between Niclosamide and PTEN-induced Putative Kinase 1.....	13
1.3.3 Limitations of Niclosamide.....	14
1.4 Drug Repurposing.....	14
1.4.1 The Advantages of Drug Repurposing.....	15
1.4.2 The Disadvantages of Drug Repurposing.....	15
1.5 Rational Drug Design.....	16
1.6 Computational Tools.....	16
1.6.1 BIOVIA® Discovery Studio®.....	17
1.6.2 SYBYL®-X.....	17
1.6.3 USCF Chimera® v1.12.....	17
1.6.4 BIOVIA® Accelrys Draw® v.4.1.....	18

1.6.5 LigandScout®	18
1.6.6 ZINCPharmer®	18
1.6.7 Mona®	19
1.6.8 X-Score®	19
1.6.9 LigBuilder®	19
1.7 Aims and Objectives	20
2. Methodology	22
2.1 Selection of the PDB Crystallographic Deposition.....	22
2.2 Generation of the <i>apo</i>-receptor and Extraction of Ligands	22
2.3 Conformational Analysis	24
2.3.1 Generation of Niclosamide Conformers.....	24
2.3.2 Calculation of the Ligand Binding Energy (LBE) (Kcal mol ⁻¹) and Ligand Binding Affinity (LBA) (pK _d).....	24
2.3.3 Identification of the Optimal Conformer.....	25
2.4 Virtual Screening	25
2.4.1 Consensus Pharmacophore Generation	25
2.4.2 Hit Molecule Generation	26
2.4.3 Filtration of Hits	27
2.4.4 Protomol Generation	28
2.5 De Novo Approach	29
2.5.1 The Generation of 2D and 3D Topology Maps.....	29

2.5.2 Seed Generation.....	30
2.5.3 <i>De Novo</i> Design.....	31
2.5.4 Filtration of Results	32
3. Results	34
3.1 Results Obtained from Virtual Screening.....	34
3.1.1 Identification of the Optimal Niclosamide Conformer	34
3.1.2 The Structure of the Optimal Niclosamide Conformer	35
3.1.3 Consensus Pharmacophore	35
3.1.4 Affinity of the Molecules obtained through Virtual Screening for the Modelled PINK1 Protomol.....	36
3.2 Results Obtained from <i>De Novo</i> Approach	40
3.2.1 Seeds Generated from the Selected Optimal Conformer	40
3.2.2 Ligands Generated from the Seed Structures	42
4. Discussion	55
References.....	62
Appendix A: Ethics Approval.....	69
Addendum	70

List of Tables

Table 2.1: A table showing parameters set to generate hit molecules according to the Rule of 3 for lead-likeness.	27
Table 3.1: A table showing the top six molecules obtained through virtual screening. Images rendered in Discovery Studio ^{®1}	37
Table 3.2: A table showing the five seed structures created from the de novo approach, along with the 2D structure indicating the exact loci allocated for growth, that is, the H.sp.c atom. Images rendered in Discovery Studio ^{®1}	40
Table 3.3: A table comparing the structures of the ligands having the highest and lowest affinity towards the PINK1 receptor obtained from Seed 1. Images rendered in Discovery Studio ^{®1}	42
Table 3.4: A table comparing the structures of the ligands having the highest and lowest affinity towards the PINK1 receptor obtained from Seed 2. Images rendered in Discovery Studio ^{®1}	43
Table 3.5: A table comparing the structures of the ligands having the highest and lowest affinity towards the PINK1 receptor obtained from Seed 3. Images rendered in Discovery Studio ^{®1}	46
Table 3.6: A table comparing the structures of the ligands having the highest and lowest affinity towards the PINK1 receptor obtained from Seed 4. Images rendered in Discovery Studio ^{®1}	48
Table 3.7: A table comparing the structures of the ligands having the highest and lowest affinity towards the PINK1 receptor obtained from Seed 5. Images rendered in Discovery Studio ^{®1}	51

Table 4.1: 2D representations of the 3 optimal de novo designed molecules together with their respective pharmacophores P1 and P2. P1 is the user designed seed structure. Images rendered in Discovery Studio ^{®1}	57
---	----

List of Figures

Figure 1.1: The structure of Ubiquitin obtained by X-ray diffraction with a resolution of 3.6 Å rendered in UCSF Chimera® (Pettersen et al., 2004) based on PDB 1R4N (Walden et al., 2003).....	6
Figure 1.2: The structure of Parkin E3 ligase obtained by X-ray diffraction with a resolution of 2 Å rendered in UCSF Chimera® (Pettersen et al., 2004) based on PDB 4I1H (Riley et al., 2013).	6
Figure 1.3: The structure of TRAP-1 obtained by X-ray diffraction with a resolution of 2.59 Å rendered in UCSF Chimera® (Pettersen et al., 2004) based on PDB 7C05 (Darong et al., 2020).	7
Figure 1.4: The structure of BCL-xL obtained by X-ray diffraction with a resolution of 1.95 Å rendered in UCSF Chimera® (Pettersen et al., 2004) based on PDB 1R2D (Manion et al., 2003).....	8
Figure 1.5: The structure of HtrA2 obtained by X-ray diffraction with a resolution of 2 Å rendered in UCSF Chimera® (Pettersen et al., 2004) based on PDB 1LCY (Li et al., 2002).	9
Figure 1.6: The structure of PINK-1 obtained by X-ray diffraction with a resolution of 2.53 Å rendered in UCSF Chimera® (Pettersen et al., 2004) based on PDB 5YJ9 (Okatsu et al., 2018).....	11
Figure 1.7: The structure of niclosamide rendered in Discovery Studio®	13
Figure 2.1: The structure of the cognate small molecule ANP601 as described in PDB crystallographic deposition 5YJ9 (Okatsu et al., 2018) observed in 3D and 2D respectively. Images rendered in Discovery Studio®	23

Figure 2.2: The structure of the apo-PINK1 receptor as described in PDB crystallographic deposition 5YJ9 (Okatsu et al., 2018) rendered in Discovery Studio [®]	23
Figure 2.3: PDB 5YJ9 (Okatsu et al., 2018) in macromolecular view rendered in LigandScout [®] (Wolber & Langer, 2005).	26
Figure 2.4: The protomol of the PINK1 receptor as described in PDB crystallographic deposition 5YJ9 (Okatsu et al., 2018) rendered in SYBYL-X [®] (Ash, 1997).	28
Figure 2.5: The 2D topology map generated that represents the interactions between the optimal niclosamide conformer and PINK1 LBP rendered in Discovery Studio ^{®1} . .	30
Figure 3.1: The structure of the optimal niclosamide conformer shown in 3D and 2D respectively. Images rendered in Discovery Studio ^{®1}	35
Figure 3.2: The pharmacophoric features of the bioactive small molecule ANP601 within PINK1 receptor superimposed onto the optimal niclosamide conformer rendered LigandScout [®] (Wolber & Langer, 2005).	35
Figure 3.3: Consensus pharmacophore incorporating the critical pharmacophoric features of the optimal conformer of niclosamide and those of the crystallographically described ANP601 represented in PDB 5YJ9 (Okatsu et al., 2018) rendered in LigandScout [®] (Wolber & Langer, 2005).	36
Figure 4.1: Critical interactions forged between ANP601 (i) and the optimal niclosamide conformer (ii) to the PINK1 LBP. Images rendered in Discovery Studio ^{®1}	59

List of Graphs

Graph 3.1: A line graph showing LBE in Kcal mol⁻¹ on the left y-axis and LBA in pKd on the right y-axis, and the conformer number on the x-axis. 34

List of Appendices

Appendix A: Ethics Approval.....	69
---	-----------

Glossary

Agonist	A ligand that activates the receptor.
Antagonist	A ligand that inhibits the receptor.
<i>apo</i>	A receptor in its unbound form.
Conformational analysis	The spatial arrangement of a group of atoms that are essential for the biological activity brought about.
Consensus pharmacophore	The essential atoms or molecular features required for the interaction between the ligand and the receptor.
<i>in silico</i>	The activity is performed on the computer or simulated computationally.
Lead molecule	A chemical compound that shows the desired biological and pharmacological activity and is therefore a good candidate for drug development.

List of Abbreviations

ADME	Absorption, Distribution, Metabolism and Excretion
ATP	Adenosine Triphosphate
COMT	Catechol-O-methyltransferase
CTR	Carboxy-terminal Region
DBS	Deep Brain Stimulation
HBA	Hydrogen Bond Acceptor
HBD	Hydrogen Bond Donor
HtrA2	High Temperature Requirement A2
LBP	Ligand Binding Pocket
NMDA	<i>N</i> -methyl-D-aspartic acid
NMR	Nuclear Magnetic Resonance
PD	Parkinson's Disease
PDB	Protein Data Bank
PINK-1	PTEN-induced Putative Kinase 1
TRAP-1	TNF Receptor-associated Protein 1
Ub	Ubiquitin
UbL	Ubiquitin Like

VMD Visual Molecular Dynamics

VS Virtual screening

Chapter 1:

Introduction

1. Introduction

Currently, Parkinson's disease (PD) affects approximately 4-20 per 100,000 individuals. It is twice more likely to occur in men than in women and this incidence increases with age (Chaudhuri *et al.*, 2011; Poewe *et al.*, 2017). The primary molecule for PD treatment is levodopa; however, its use is limited due to the development of motor complications, such as motor response oscillations and drug-induced dyskinesia (Chaudhuri *et al.*, 2011).

1.1 Current Treatments for Parkinson's Disease

Most patients suffering from PD are treated with levodopa, which is used to increase dopamine concentration within the brain, since this is depleted as the disease progresses. Levodopa, being a precursor of dopamine, is converted into dopamine as it is able to cross the blood brain barrier, however is also converted peripherally thus decarboxylase inhibitors are used to reduce unwanted side effects. Catechol-O-methyltransferase (COMT) inhibitors are also used to increase the bioavailability of levodopa (Chaudhuri *et al.*, 2011; Poewe *et al.*, 2017).

The major limitation of this treatment is that, the longer a patient is on levodopa, the more likely motor complications will occur, since levodopa has a relatively short half-life. Studies have suggested that dopamine agonists, such as ropinirole and pramipexole, can be used to prevent or delay these complications. Another limitation for this treatment is that patients with young-onset PD are not advised to start levodopa treatment immediately due to these motor complications (Chaudhuri *et al.*, 2011; Poewe *et al.*, 2017).

For the treatment of motor fluctuations and dyskinesia in patients with advanced PD, a therapy using high-frequency (100-200Hz) electrical stimulation has been established that involves the surgical implantation of an electrode into the brain tissue which will generate electrical impulses to control abnormal brain activity. This procedure is known as ‘Deep Brain Stimulation’ (DBS). The main limitation for this treatment is that it cannot be used for every patient. Patients who have not responded to levodopa treatment will not respond to DBS. In addition to this, patients with PD complications such as dementia, major depression and acute psychosis will also not respond (Poewe *et al.*, 2017; Radhakrishnan & Goyal, 2018).

Ongoing clinical trials testing the efficacies of molecules that are capable of modifying the disease progression are tested on animals that have been given dopaminergic toxins to mimic Parkinsonian-like symptoms. This poses a complication due to the difference in anatomy and disease pathology, as a number of other neurotransmitters are involved in human PD (Gelati & Di Giovanni, 2010).

1.1 PTEN-induced Putative Kinase 1 Receptor

One avenue for the novel drug design of a molecule that is capable of modifying the PD course is the ‘PTEN-induced Putative Kinase 1’ (PINK1) receptor. This receptor is found in the mitochondria since it is a mitochondrial kinase which consists of 581 amino acids. It encodes for a serine/threonine kinase domain, a transmembrane domain and a mitochondrial targeting sequence (Triplett *et al.*, 2015). PINK1 mutations are linked to autosomal recessive PD due to a defect in the mitochondrial energy metabolism and oxidative stress (Chaudhuri *et al.*, 2011; Song *et al.*, 2013). Studies have shown that mitochondrial dysfunction which would lead to PINK1 deficiency,

ultimately results in decreased dopamine levels mainly in the striatum, which is a characteristic of PD (Beilina *et al.*, 2005; Lu *et al.*, 2018; Zhi *et al.*, 2019).

The PINK1 receptor is able to mediate the phosphorylation of the complex I subunit NdufA10, in healthy mitochondria, in order to adjust the overall adenosine triphosphate (ATP) production. This receptor also protects the cells from Ca^{2+} induced cell death by regulating the mitochondrial $\text{Na}^+/\text{Ca}^{2+}$ efflux (Leites & Morais, 2018).

Studies have shown that PINK1, along with a cytosolic E3 ubiquitin (Ub) ligase, or Parkin, are involved in the selective autophagy degradation of damaged mitochondria, also known as mitophagy (Vincow *et al.*, 2013). Mitophagy is the process whereby one may maintain a healthy mitochondrial network by employing cells to identify and tag dysfunctional mitochondria for future degradation (Leites & Morais, 2018; von Stockum *et al.*, 2018). This process starts off with damaged organelles and protein aggregates being identified by PINK1 which then signals Parkin to tag those identified with Ub. PINK1 is then imported to the inner mitochondrial membrane, where cleavage of the *N*-terminal mitochondrial targeting sequence is carried out by the mitochondrial protease. Mitophagy is initiated once PINK1 stabilizes on the outer mitochondrial membrane either due to accumulation of damaged proteins or when the membrane potential decreases (Lazarou *et al.*, 2015; Pickrell & Youle, 2015; Triplett *et al.*, 2015; Leites & Morais, 2018; von Stockum *et al.*, 2018). A portion of PINK1 is degraded by the proteasome in the cytosol and another portion remains in the cytoplasm where it has been implicated that it is involved in various pathways including; AKT signal transduction, synaptic plasticity and dopamine synthesis (Lazarou *et al.*, 2015; Triplett *et al.*, 2015).

Mutations, either in the Parkin gene or in PINK1 may disrupt this process leading to accumulation of damaged proteins, which has been linked to numerous neurodegenerative disorders such as PD (Gies *et al.*, 2010).

1.2.1 Endogenous Agonists of PTEN-induced Putative Kinase 1

Ub (Figure 1.1) is a primary endogenous agonist of PINK1 as it binds to it and is phosphorylated. This newly phosphorylated Ub promotes phosphorylation of the Ub-like (UBL) domain on Parkin (Figure 1.2), by PINK1. This leads to Parkin being enzymatically activated and helps attach other Ub molecules to neighbouring proteins which need to be removed, and thus the process of autophagy begins (Daou & Sicheri, 2017). Parkin is able to form mitochondria-derived vesicles when phosphorylated by PINK1 thus facilitating the survival of healthy mitochondria (Leites & Morais, 2018).



Figure 1.1: The structure of Ubiquitin obtained by X-ray diffraction with a resolution of 3.6 Å rendered in USCF Chimera[®] (Pettersen *et al.*, 2004) based on PDB 1R4N (Walden *et al.*, 2003).

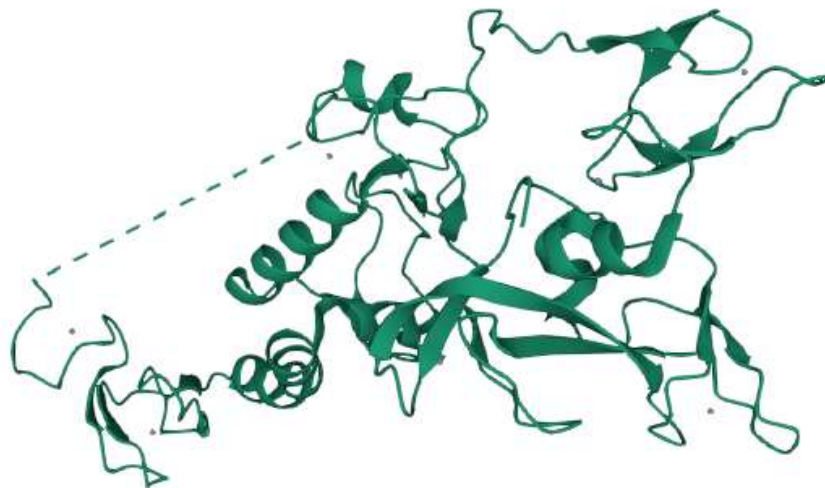


Figure 1.2: The structure of Parkin E3 ligase obtained by X-ray diffraction with a resolution of 2 Å rendered in USCF Chimera[®] (Pettersen *et al.*, 2004) based on PDB 4I1H (Riley *et al.*, 2013).

Studies have shown that a heat shock protein, known as TNF receptor-associated protein 1 (TRAP-1) (Figure 1.3) is capable of agonizing PINK1 that results in phosphorylation of the protein. This process results in a suppression of cytochrome C release from the mitochondria, thus protecting PINK1 against oxidative stress-induced apoptosis (Pridgeon *et al.*, 2007).



Figure 1.3: The structure of TRAP-1 obtained by X-ray diffraction with a resolution of 2.59 Å rendered in UCSF Chimera[®] (Pettersen *et al.*, 2004) based on PDB 7C05 (Darong *et al.*, 2020).

Physiologically similar to TRAP-1, the proteins BCL-xL shown in figure 1.4 and high temperature requirement HtrA2 show in figure 1.5 also provide cellular protection once phosphorylated by PINK1 (Leites & Morais, 2018). A reduction in HtrA2 phosphorylation in patients with a PINK1 mutation implies that the PINK1 receptor has an essential role in regulating the proteolytic activity of HtrA2 thus promoting cell survival as a result of mitochondrial damage (Strauss *et al.*, 2005; Plun-Favreau *et al.*, 2007).

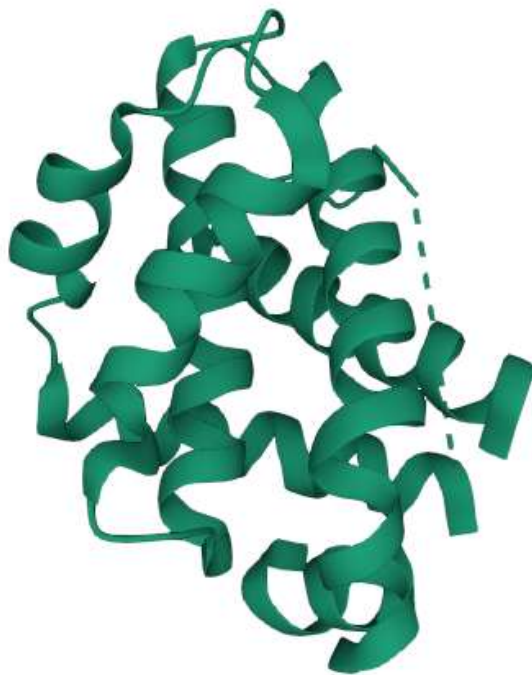


Figure 1.4: The structure of BCL-xL obtained by X-ray diffraction with a resolution of 1.95 Å rendered in USCF Chimera[®] (Pettersen *et al.*, 2004) based on PDB 1R2D (Manion *et al.*, 2003).

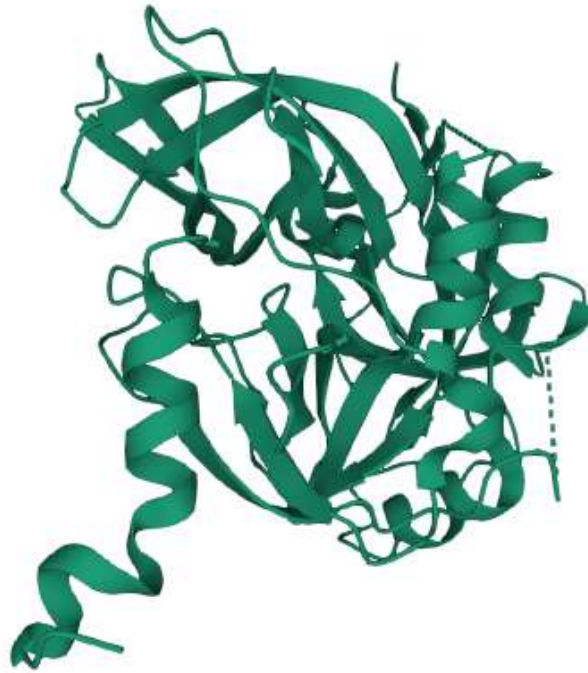


Figure 1.5: The structure of HtrA2 obtained by X-ray diffraction with a resolution of 2 Å rendered in UCSF Chimera[®] (Pettersen *et al.*, 2004) based on PDB 1LCY (Li *et al.*, 2002).

1.2.2 The Structure of PTEN-induced Putative Kinase 1

As previously described, PINK1 (Figure 1.6) is a mitochondrial kinase, meaning it also has a kinase domain where phosphorylation can occur. The kinase domain consists of amino- and carboxy- terminal lobes, that is N- and C- terminals respectively (Daou & Sicheiri, 2017). Between these two terminals a cleft is formed and an ATP analogue is bound. This binding occurs due to the adenine ring of the ATP analogue binding to the hydrophobic pocket, whilst the triphosphate group and two co-ordinated magnesium ions are interacting with the catalytic hydrophilic residues (Okatsu *et al.*, 2018). The PINK1 receptor is unique since it has three amino acid sequences known as insertions and also has a carboxy-terminal region (CTR) domain which is only found on the PINK1 receptor (Daou & Sicheiri, 2017).

The N-terminal of the PINK1 receptor contains five-stranded antiparallel α -sheet, an α -helix and three PINK-1 specific insertions. A loop that contains acidic amino-acid residues is formed by insertion 1 (Okatsu *et al.*, 2018). The role of insertion 1 is still unknown; however, studies have shown that the enzymatic activity of PINK1 is regulated by insertion 2. This insertion is made up of a β -strand and an α -helix, which together pack in a vicinity of a conserved helix, thus reconfiguring the N-lobe. The third insertion is involved in substrate binding. It helps to form a contact surface between the enzyme and the substrate (Daou & Sicheri, 2017).

On the other hand, the C-terminal is mainly composed of α D- α I, which contains the sustained HRD motif (³³⁵His-Arg-Asp³³⁷), also known as the catalytic loop, and the activation loop. The activation loop is characterised by the region between DFG (³⁵⁹Asp-Phe-Gly³⁶¹) and the APE motifs (³⁹⁰Ala-Pro-Glu³⁹²) (Okatsu *et al.*, 2018). It is further configured by forming a globular protrusion at the back of the kinase domain, that is, where the CTR domain is found, which has three α -helices. The CTR domain and the C-terminal are inseparable due to the extensive hydrophobic interactions that bind them together (Daou & Sicheri, 2017; Okatsu *et al.*, 2018).

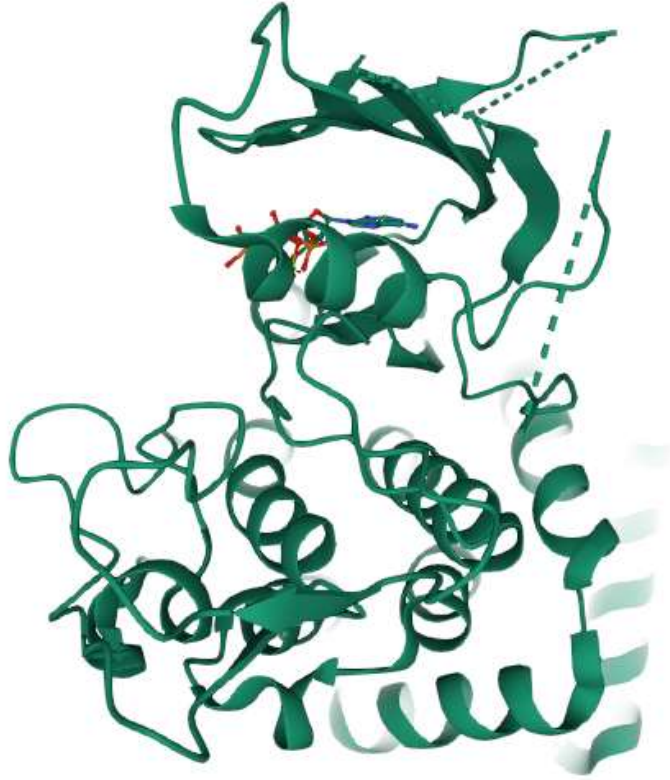


Figure 1.6: The structure of PINK-1 obtained by X-ray diffraction with a resolution of 2.53 Å rendered in UCSF Chimera[®] (Pettersen *et al.*, 2004) based on PDB 5YJ9 (Okatsu *et al.*, 2018).

1.2.3 The Requirements of Binding to PTEN-induced Putative Kinase 1

The primary residues for substrate specificity are allocated within the P-loop, α C, α D, α F, α G, as well as the activation loop. These specifications were revealed by complex structures such as protein kinase A and protein kinase C. The structural elements described above, are able to form a groove which can accommodate a substrate peptide. This groove is approximately 15Å-wide. Another two grooves are located in the extracellular signal-regulated kinase 2 and LIM domain kinase 1, which have a width of 22 Å and 24 Å respectively, that accommodate globular proteins along with ribosomal S6 kinase 1 and cofilin/ADF (Okatsu *et al.*, 2018).

Studies have been carried out on the binding between PINK1 and Ub. It has been shown that a probable PINK1 binding surface on Ub is positively charged and so corresponds to the negatively charged binding surface found on PINK1 (Okatsu *et al.*, 2018).

1.2.4 Antagonists of PTEN-induced Putative Kinase 1

Literature has showed no possible antagonists of PINK1 (Beilina *et al.*, 2005; Shan *et al.*, 2009), however indirect ones, that is PINK1 expression being reduced due to inhibition of another receptor are being studied. As an example, studies showed the receptor N-Methyl-D-aspartic acid (NMDA) being blocked by either a calcium channel blocker, dizocilpine, or by D-APV. This inhibition causes a reduction effect on PINK1 expression, which will reduce oxygen-glucose deprivation induced neuronal death. This study is not yet at the clinical testing phase (Shan *et al.*, 2009).

1.3 Niclosamide as a PTEN-induced Putative Kinase 1 Agonist

1.3.2 Literature on Niclosamide

The Universities of Cardiff and Dundee in the United Kingdom identified the anthelmintic drug, niclosamide (Figure 1.7) and its derivatives, as being capable of agonising PINK1. More specifically, the analogue labelled AM85 has more capability of being a PINK1 agonist. It was found that for molecules to activate this receptor, they have to be small. Niclosamide has been used in humans to treat tapeworm infections for over half a century, showing that it is safe to use, and no severe side effects have been noted (Barini *et al.*, 2018).

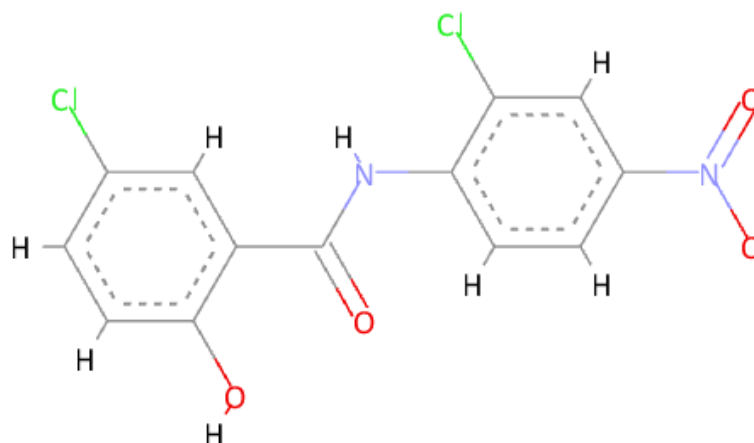


Figure 1.7: The structure of niclosamide rendered in Discovery Studio^{®1}.

Studies suggest that niclosamide induces autophagy by preventing large Ub-containing aggregates from forming; therefore accumulation of damaged proteins does not occur. It is hypothesised that niclosamide may be able to induce clearance of such proteins, which would decrease the pathogenesis of neurodegenerative diseases (Gies *et al.*, 2010).

1.3.2 Interactions between Niclosamide and PTEN-induced Putative Kinase 1

The anthelmintic drug niclosamide is able to indirectly activate PINK1 by preventing ATP from being produced, thus causing the phenomenon known as mitochondrial depolarization, that is loss of the mitochondrial membrane potential. It was noted that this process is reversible after removing niclosamide from the cell media. This phenomenon was observed whilst treating parkin-overexpressing HeLa cells that

¹ Biovia. Biovia Discovery Studio [Internet], United States of America; 2018 [cited 2021 Mar 16]. Available from: <http://accelrys.com/products/collaborative-science/biovia-discovery-studio/>

express PINK1 endogenously, with niclosamide (Kadri *et al.*, 2018; Lambourne & Mehellou, 2018).

Niclosamide, therefore, has an indirect approach which is mediated by its ability to uncouple mitochondria. This activation of PINK1 results in an enhancing action of PINK1 which has been shown to halt neurodegeneration and therefore is a key step in slowing down the progression of PD (Barini *et al.*, 2018; Pinto, 2018).

1.3.3 Limitations of Niclosamide

A limitation of niclosamide is that it can manipulate many signalling pathways both *in vivo* and in cells, and thus is a disadvantage from a drug repurposing perspective. Studies have also suggested that niclosamide is poorly soluble and has inefficient absorption; however this limitation can be overcome when using pro-drugs with improved drug-like properties. Research is still ongoing as to evaluate the brain penetration properties of the pro-drugs (Lambourne & Mehellou, 2018).

1.4 Drug Repurposing

Drug repurposing is the process whereby drugs which are already marketed, and thus have been studied with regards to safety, are further investigated in terms of efficacy in another disease other than the one originally developed for. As an example, niclosamide which is already on the market and approved for human use as an anthelmintic drug, is being investigated for the management of PD (Strittmatter, 2014). Drug repurposing is possible since clinically used drugs are non-selective to a single

target. This concept may be the solution to develop drugs aim at treating rare diseases (Lipinski, 2011).

1.4.1 The Advantages of Drug Repurposing

The main advantage of drug repurposing is the lack of completeness in the drug-target interaction profiles and therefore new indications for an already-approved drug can be discovered. On account that the drug is already approved and therefore is safe, one can further carry out phase I and phase II clinical trials which mainly focus on safety to further investigate and establish the maximum dose. On the other hand, phase III which focuses on efficacy and phase IV focusing on post-marketing surveillance, need to be carried out to give an additional understanding of how the drug is tolerated in the long-term. Therefore resources are saved resulting in the repurposed drug being put on the market faster. With drug repurposing, the life of successful drug franchises is prolonged (Opera & Mestres, 2014; Pantziarka *et al.*, 2014).

1.4.2 The Disadvantages of Drug Repurposing

Drug repurposing does have some limitations, mainly when it comes to debating intellectual property right and economic incentives as the originator company holds the drug's patent, whereas another company has repurposed the drug. From another perspective, the repurposed drug may have a good affinity only when in access of the original registration of the drug (Pantziarka *et al.*, 2014).

1.5 Rational Drug Design

Rational drug design can be divided into two categories. The first being, developing small molecules with a desired affinity towards a specific target which has been already studied and therefore knowledge about it is known. The other approach is to develop small molecules with a limited affinity towards a target, which may or may not have been studied already. These unknown targets can be studied by using computational tools, and treating them with a known drug, and thus studying the global gene expression of the target (Reddy, 2007; Mandal *et al.*, 2009).

The mentioned methods of rational drug design need to evaluate aspects, such as hydrophilicity and lipophilicity, once the target has been identified. This further research would help to reduce side effects or even eliminate the disease. Furthermore, the advances made specifically in X-ray crystallography and nuclear magnetic resonance (NMR) has made it possible to precisely predict an effect a specific lead molecule can have on a target, this leads to a shortened discovery time (Reddy, 2007; Mandal *et al.*, 2009).

1.6 Computational Tools

The advancement in computational procedures is nowadays an essential step in the drug discovery process, since it manages to prompt structural and functional properties of biological macromolecules, and can be drawn in a 3-dimensional manner (Parenti & Rastelli, 2012).

1.6.1 BIOVIA® Discovery Studio®

With Discovery Studio®, resources such as money and time can be diminished since it allows the investigation of a hypothesis by means of *in silico* testing. Through *in silico* testing, several targets can be explored and therefore new targets can be easily found. This programme also allows the user to share findings with colleagues, and hence is easier to receive feedback on one's research. ¹

1.6.2 SYBYL®-X

This programme allows one to view a molecule from a 2-dimensional view to a 3-dimensional one, and hence helps researchers to understand better aspects of the molecule such as absorption, distribution, metabolism and elimination (ADME), thus one can model the molecule. SYBYL®-X carries out ligand based virtual screening (VS) which is done by docking the molecule into the generated protomol and analysing its affinity towards the target receptor (Ash, 1997).

1.6.3 USCF Chimera® v1.12

This specific computational tool is used to develop high-quality images or animations of a molecule. Hence it is used for an interactive visualization of structures which helps researches to interpret a molecule from a better perspective (Pettersen *et al.*, 2004).

¹ Biovia. Biovia Discovery Studio [Internet], United States of America; 2018 [cited 2021 Mar 16]. Available from: <http://accelrys.com/products/collaborative-science/biovia-discovery-studio/>

1.6.4 BIOVIA[®] Accelrys Draw[®] v.4.1

BIOVIA Draw[®] is a software used for drawing and/or editing of molecular bonds or complex structures easily. It also includes features such as archiving information and collaborative searches. This version includes as well a biological sequence editor.²

1.6.5 LigandScout[®]

Ligand-based VS can be performed on LigandScout[®] as different chemical conformations and tautomers can be introduced in the software with the added benefit of fast calculations which is not time consuming (Wolber & Langer, 2005).

1.6.6 ZINCPharmer[®]

ZINCPharmer[®] uses pharmacophores to search through the online ZINC database containing purchasable compounds that can identify potential lead compounds by superimposing both pharmacophores. A pharmacophore is defined as the essential features of a molecule which are critical for any interactions; this includes the spatial arrangement of atoms. ZINCPharmer[®] is a fast tool used to construct and refine pharmacophores, with the ability to view results immediately and download them for off line analysis (Koes & Camacho, 2012).

² Biovia. Biovia Draw [Internet], United States of America; 2018 [cited 2021 Mar 16]. Available from: <http://accelrys.com/products/collaborative-science/biovia-draw>

1.6.7 Mona[®]

Mona allows for analysis of a large collection of molecules including visualization, filtering and clustering of molecules based on similarity. Consistency and correctness is ensured as it is based on a stable underlying cheminformatics library therefore no expert knowledge of the subject is needed to operate this software (Hilbig & Rarey, 2015).

1.6.8 X-Score[®]

This software calculates the ligand binding energy and ligand binding affinities of ligands towards a target receptor by implementing a ‘scoring function’, taking into account the energetic factors essential for the protein-ligand binding (Wang *et al.*, 2003).

1.6.9 LigBuilder[®]

LigBuilder[®] was developed to aid structure-based drug design by adding organic fragments to a target protein by using one of the algorithms either GROW or LINK. The obtained molecules are further analysed with respect to the binding affinities towards the target receptor which is estimated by an empirical scoring function, in addition to evaluating the bioavailabilities based on a set of chemical rules (Wang *et al.*, 2000).

1.7 Aims and Objectives

This literature review has reinforced the fact that existing treatments for the management of PD are very limited and that there is ample scope for continued research into this field (Galati & Di Giovanni, 2010). Novel and hitherto undiscovered targets may represent the way forward, and the PINK1 receptor identified in this literature review represents a good example and may be used in novel research avenues. Literature has also shown that niclosamide, a small molecule with which we have experience as an anthelmintic, is capable of acting as an agonist at the PINK1 receptor and of slowing down progression of the disease (Barini *et al.*, 2018). The fact that niclosamide is therefore being repurposed is a further advantage owing to the fact that there is a prior knowledge that niclosamide is orally bioavailable³ and non-toxic (Ye *et al.*, 2014; Barini *et al.*, 2018).

The sum total of the data emanating from this literature review validates the execution of this study which consequently aims to repurpose the niclosamide scaffold from its traditional use as an anthelmintic agent into an anti-Parkinsonian drug. Specifically, the critical interactions forged between the niclosamide and the PINK1 ligand binding pocket (LBP) will be analysed and used in the identification and *de novo* design of niclosamide analogues capable of superior PINK1 modulation.

³ National Cancer Institute. Niclosamide [Internet], United States of America: NCIThesisaurus; 2018 [cited 2020 Mar 17]. Available from: https://ncit.nci.nih.gov/ncitbrowser/ConceptReport.jsp?dictionary=NCI_Thesaurus&ns=NCI_Thesaurus&code=C66240

Chapter 2:

Methodology

2. Methodology

2.1 Selection of the PDB Crystallographic Deposition

The protein data bank (PDB) 5YJ9 (Okatsu *et al.*, 2018) was used as a template in all subsequent procedures carried out in this study as it describes the PINK1: ANP small molecule inhibitor complex in an attempt to identify other molecules capable of agonising the PINK1 receptor.

The PDB 5YJ9 (Okatsu *et al.*, 2018) was resolved crystallographically to 2.53Å which provides information about the molecule, including its proteins and nucleic acids, and most importantly regarding its 3D structure allowing users to visualize the molecule.

2.2 Generation of the *apo*-receptor and Extraction of Ligands

The PDB crystallographic deposition 5YJ9 (Okatsu *et al.*, 2018) was loaded onto SYBYL-X® (Ash, 1997) and the small molecule ANP601 was extracted from its LBP and saved as a *.mol2* file. This extraction generated the *apo*-PINK1 receptor which was saved as a *.pdb* file. Molecular modelling of niclosamide was carried out in SYBYL-X® (Ash, 1997) and saved as a *.mol2* file.

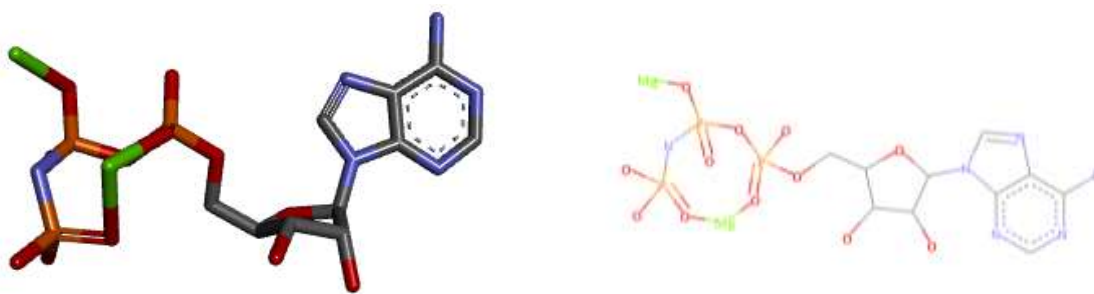


Figure 2.1: The structure of the cognate small molecule ANP601 as described in PDB crystallographic deposition 5YJ9 (Okatsu *et al.*, 2018) observed in 3D and 2D respectively. Images rendered in Discovery Studio^{®1}.

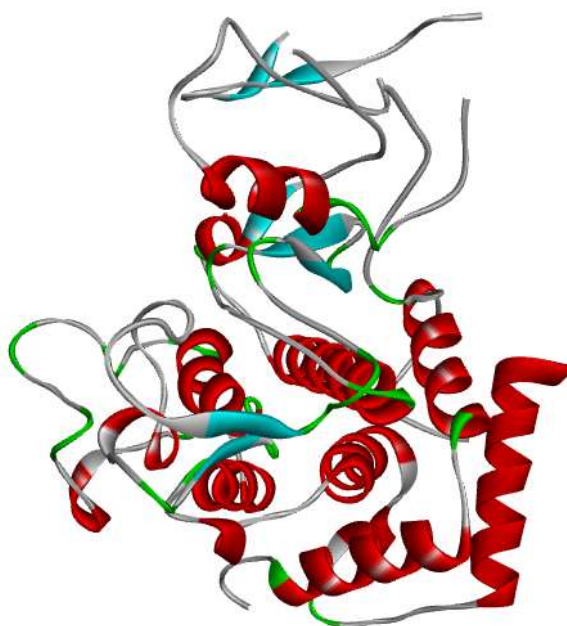


Figure 2.2: The structure of the *apo*-PINK1 receptor as described in PDB crystallographic deposition 5YJ9 (Okatsu *et al.*, 2018) rendered in Discovery Studio^{®1}.

¹ Biovia. Biovia Discovery Studio [Internet], United States of America; 2018 [cited 2021 Mar 16]. Available from: <http://accelrys.com/products/collaborative-science/biovia-discovery-studio/>

2.3 Conformational Analysis

2.3.1 Generation of Niclosamide Conformers

No previous information regarding the binding of niclosamide within the PINK1 LBP was available therefore the similarity suite function of SYBYL-X[®] (Ash, 1997) was utilized to generate different niclosamide conformers. This was carried out by docking the modelled niclosamide molecule into the *apo*-PINK1 receptor using ANP601 as a template allowing single bond and ring rotations within LBP.

A total of twenty conformers were generated each representing a possible orientation that niclosamide can occupy within the PINK1 LBP. Each conformer was isolated and saved as a *.mol2* file.

2.3.2 Calculation of the Ligand Binding Energy (LBE) (Kcal mol⁻¹) and Ligand Binding Affinity (LBA) (pK_d)

Using SYBYL-X[®] (Ash, 1997), the ligand binding energy (LBE) of all twenty conformers was calculated and was expressed as Kcal mol⁻¹. Molecules with low energy tend to be more stable; therefore a low LBE is an essential property when identifying the optimal conformer.

The ligand binding affinity (LBA) was calculated using X-Score[®] (Wang *et al.*, 2002) by calculating the affinity between the *apo*-PINK1 receptor and each of the twenty niclosamide conformers, expressed in pK_d. A high pK_d value represents great affinity of the ligand to the LBP.

The LBE and LBA of ANP601 within the *apo*-PINK1 receptor was also calculated and used as a reference. A spreadsheet containing all values generated from each conformer was compiled.

2.3.3 Identification of the Optimal Conformer

A line graph was plotted with both LBE (Kcal mol⁻¹) and LBA (pK_D) on the y-axis against conformer number on the x-axis. More specifically the LBE (Kcal mol⁻¹) was plotted on the left y-axis and the LBA (pK_D) on the right y-axis. The optimal conformer was obtained from this line graph based on the assumption that it is the molecule with the highest affinity (pK_d) and which is most energetically stable.

2.4 Virtual Screening

2.4.1 Consensus Pharmacophore Generation

The PDB crystallographic deposition 5YJ9 (Okatsu *et al.*, 2018) was loaded onto LigandScout[®] (Wolber & Langer, 2005) and displayed using the macromolecular view feature. A structure-based pharmacophore was generated using the alignment perspective option that describes the spatial arrangement of ANP601 within the PINK1 LBP.

The consensus pharmacophore was created to guide virtual screening in this study by superimposing the optimal niclosamide conformer and the bioactive small molecule ANP601. The consensus pharmacophore was exported as an *.sdf* file and indicates the critical interactions forged by both ANP601 and the optimal niclosamide conformer with the PINK1 LBP.

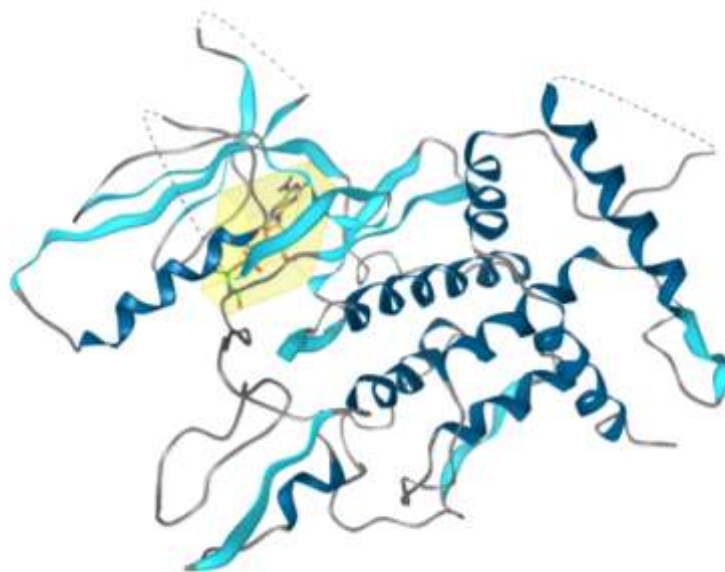


Figure 2.3: PDB 5YJ9 (Okatsu *et al.*, 2018) in macromolecular view rendered in LigandScout® (Wolber & Langer, 2005).

2.4.2 Hit Molecule Generation

The consensus pharmacophore created was used as a query structure and was read into the online database ZINCPharmer® (Koes & Camacho, 2012). Stringent rule of three (Veber *et al.*, 2002) acceptance criteria was imposed on the identified hit structures in order to ensure structural optimization would be possible from a molecular weight and rotatable bond perspective.

Table 2.1: A table showing parameters set to generate hit molecules according to the Rule of 3 for lead-likeness.

Parameter	Value
Maximum Hits per Conformer	1
Maximum Hits per Molecule	1
Maximum Total Hits	300
Max RMSD	1
Molecular Weight	1-300
Rotatable Bonds	1-3

Various purchasable databases were selected for query, including ZINC Purchasable, ZINC in Man and ZINC Natural Products, which selected analogous molecules capable of binding within the PINK1 LBP. The databases which obtained hit molecules were individually exported and saved as an *.sdf* file.

2.4.3 Filtration of Hits

Each *.sdf* file obtained from ZINCPharmer[®] (Koes & Camacho, 2012) was loaded into Mona[®] (Hilbig & Rarey, 2015) and filtered using Lipinski's Rule of 5 (Lipinski, 2011) as acceptance criteria to obtain new hit molecules with drug-like characteristics.

Each filtered database was further divided into smaller groups after filtration was completed as certain databases contained a large number of hits which would not generate the protomol in the following step. Each group was exported and saved as a *.mol2* file.

2.4.4 Protomol Generation

Using the docking suite feature in SYBYL-X[®] (Ash, 1997), a protomol was generated which represents the energetically unstable amino acids at the core of the PINK1 receptor that can be stabilized through ligand binding. This created an active site whereby ligands can be docked and examined.

The PDB crystallographic deposition 5YJ9 (Okatsu *et al.*, 2018) was docked into the docking suite and the ligand and any other substructures, including water, were extracted from the LBP, creating an *apo*-receptor. The protomol was generated once the surflex dock ligand option was selected.

The filtered hits generated in Mona[®] (Hilbig & Rarey, 2015) were loaded into the docking suite individually and the results obtained were exported to a spreadsheet. The molecules with the highest total score were selected for further optimization.

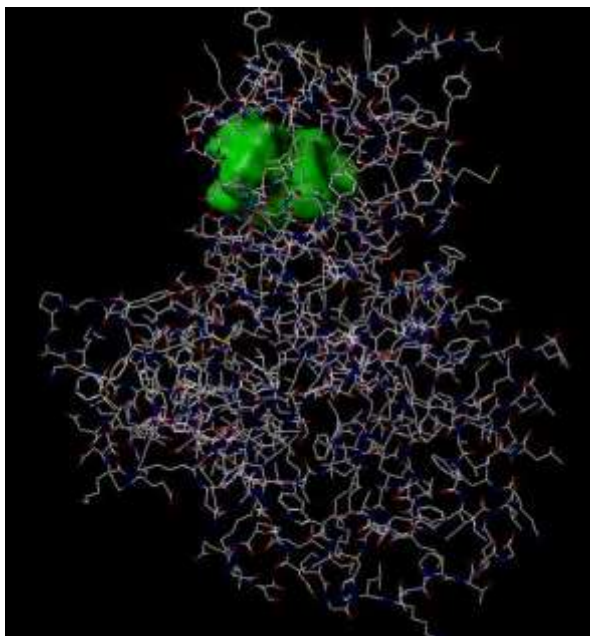


Figure 2.4: The protomol of the PINK1 receptor as described in PDB crystallographic deposition 5YJ9 (Okatsu *et al.*, 2018) rendered in SYBYL-X[®] (Ash, 1997).

2.5 *De Novo* Approach

2.5.1 The Generation of 2D and 3D Topology Maps

Prior to the topology map generation the niclosamide molecule was merged into the PINK1 receptor such that the interactions between the complex could be identified. The optimal niclosamide conformer was read into SYBYL-X[®] (Ash,1997) specifically into the *apo*-PINK1 receptor. The *apo* receptor and optimal niclosamide conformer were consequently merged into a single entity and exported in *.pdb* format for further analysis.

The optimal niclosamide conformer complexed with the PINK1 receptor was read into Discovery Studio^{®1} for the generation of a 2D topology map. The receptor-ligand interactions were displayed and the 2D map was generated and saved as an image file.

¹ Biovia. Biovia Discovery Studio [Internet], United States of America; 2018 [cited 2021 Mar 16]. Available from: <http://accelrys.com/products/collaborative-science/biovia-discovery-studio/>

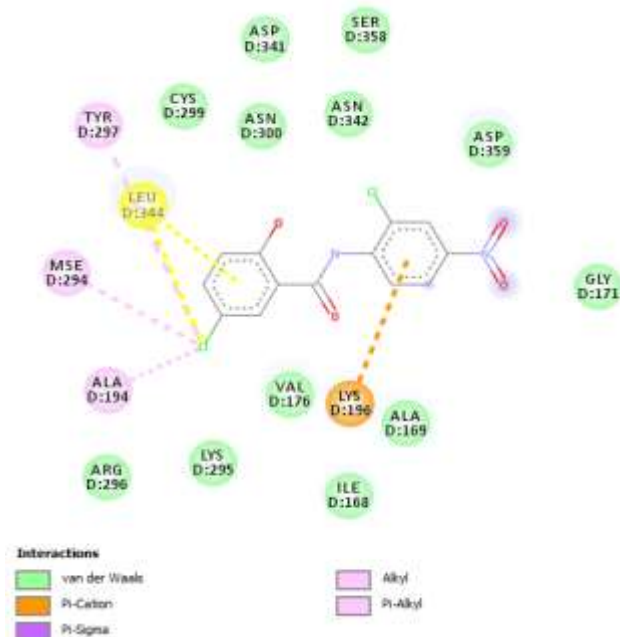


Figure 2.5: The 2D topology map generated that represents the interactions between the optimal niclosamide conformer and PINK1 LBP rendered in Discovery Studio^{®1}.

2.5.2 Seed Generation

Reference is made to the 2D topology map described in figure 2.5. Seed generation was carried out in SYBYL-X[®] (Ash, 1997) by removing any atoms shown in this map as being non-critical to binding. Structure interventions were also carried out on molecular loci shown to form unfavourable bonds with the receptor. Growing sites were designated using special hydrogen atoms (*H.spc*). This process generated a total of five seed structures.

¹ Biovia. Biovia Discovery Studio [Internet], United States of America; 2018 [cited 2021 Mar 16]. Available from: <http://accelrys.com/products/collaborative-science/biovia-discovery-studio/>

2.5.3 De Novo Design

Ligand based drug design, also known as the *de novo* approach, was carried out computationally using LigBuilder[®] (Wang *et al.*, 2000). The *apo*-PINK1 receptor and the optimal niclosamide conformer were imported into its POCKET algorithm where a ‘general pharmacophore’ and a 3D map of the LBP as circumscribed by niclosamide were generated.

The modelled seed structures were subsequently docked into the 3D LBP map generated in the POCKET module of LigBuilder[®] (Wang *et al.*, 2000) within which *de novo* molecular growth was sustained using the GROW algorithm of this software. The growing process identified the pre-designated *H.spc* atoms as anchorage sites for novel moieties from which novel molecular growth could be sustained. A parallel process was carried out using the LINK algorithm of LigBuilder[®] (Wang *et al.*, 2000). The GROW and LINK algorithms are both capable of sustaining novel molecular growth with the difference being that in the GROW algorithm only unidirectional growth is allowed while in the LINK algorithm two pre-designated fragments are linked together to form one novel entity.

The PROCESS module of LigBuilder[®] (Wang *et al.*, 2000) was used to organise and facilitate the analysis of the newly grown structures specifically this module organized all the novel structures into pharmacophorically distinct families and ranked according to LBA for the PINK1 receptor. At the end of this process, the *de novo* modelled structures were not all Lipinski rule compliant. Lipinski rule compliance was considered essential prior to further molecular analysis.

2.5.4 Filtration of Results

A double filtration process was carried out. In the first filtration, the *de novo* grown structures were filtered for Lipinski rule compliance exclusively for molecular weight and calculated log P perspective. These were the only physical chemical parameters described by the PROCESS module of LigBuilder[®] (Wang *et al.*, 2000). The structures surviving this preliminary filtration were re-filtered for hydrogen bond acceptors (HBA) and hydrogen bond donors (HBD) count using BIOVIA Draw^{®2}. This second molecular cohort was consequently considered as being Lipinski rule complaint and suitable for further analysis.

² Biovia. Biovia Draw [Internet], United States of America; 2018 [cited 2021 Mar 16]. Available from: <http://accelrys.com/products/collaborative-science/biovia-draw>

Chapter 3:

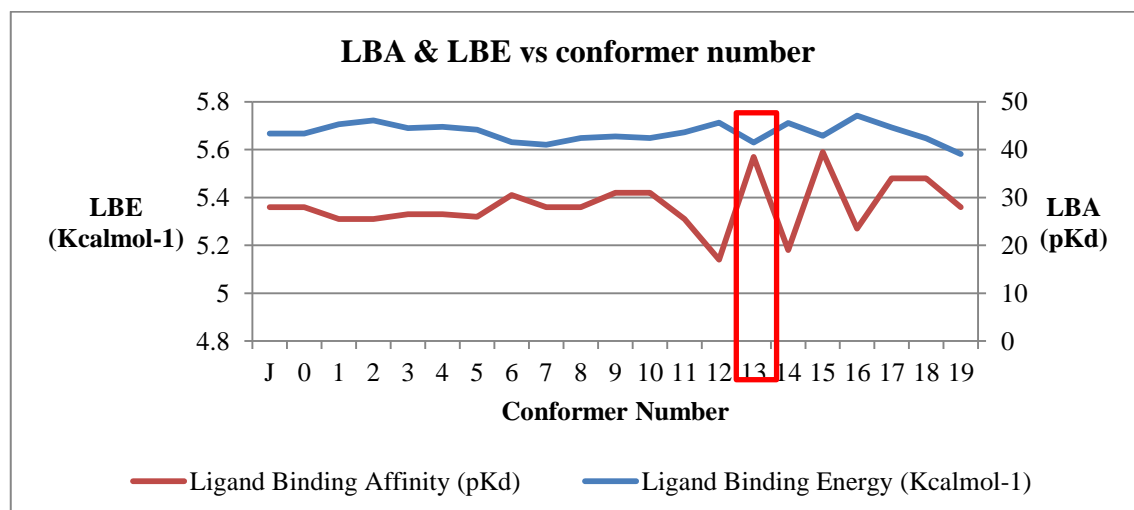
Results

3. Results

3.1 Results Obtained from Virtual Screening

3.1.1 Identification of the Optimal Niclosamide Conformer

A line graph (Graph 3.1) was plotted showing the LBE (Kcal mol^{-1}) and LBA (pK_d) of each conformer to easily identify the optimal conformer that is the conformer with a high LBA (pK_d) showing great affinity towards the receptor and a low LBE (Kcal mol^{-1}) showing good stability. The optimal conformer was identified as the fourteenth molecule, that is, conformer 13 shown in red.



Graph 3.1: A line graph showing LBE in Kcal mol^{-1} on the left y-axis and LBA in pK_d on the right y-axis, and the conformer number on the x-axis.

3.1.2 The Structure of the Optimal Niclosamide Conformer

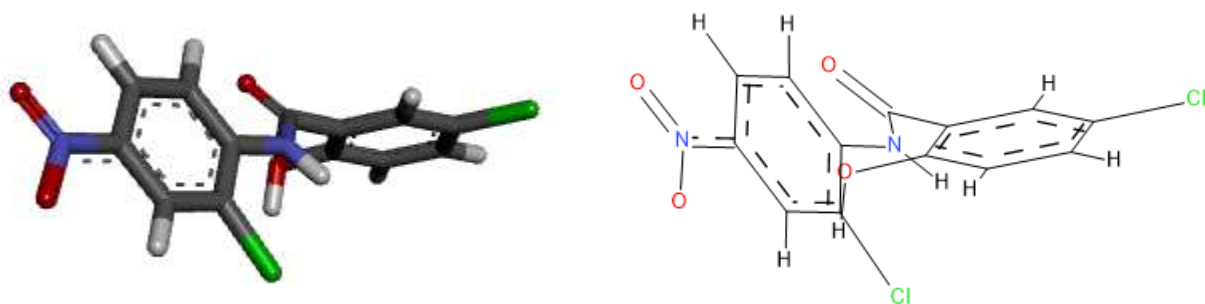


Figure 3.1: The structure of the optimal niclosamide conformer shown in 3D and 2D respectively. Images rendered in Discovery Studio^{®1}.

3.1.3 Consensus Pharmacophore

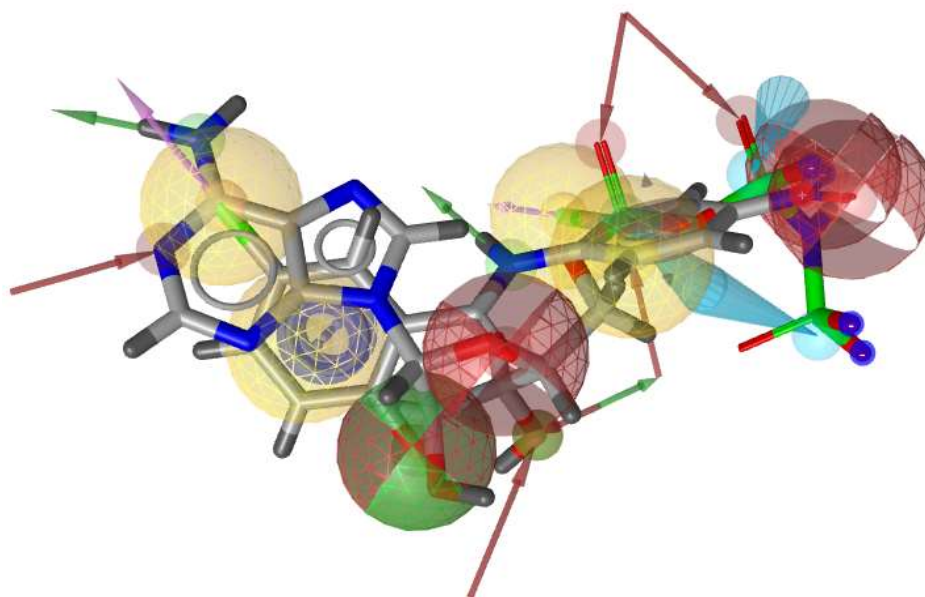


Figure 3.2: The pharmacophoric features of the bioactive small molecule ANP601 within PINK1 receptor superimposed onto the optimal niclosamide conformer rendered LigandScout[®] (Wolber & Langer, 2005).

¹ Biovia. Biovia Discovery Studio [Internet], United States of America; 2018 [cited 2021 Mar 16]. Available from: <http://accelrys.com/products/collaborative-science/biovia-discovery-studio/>

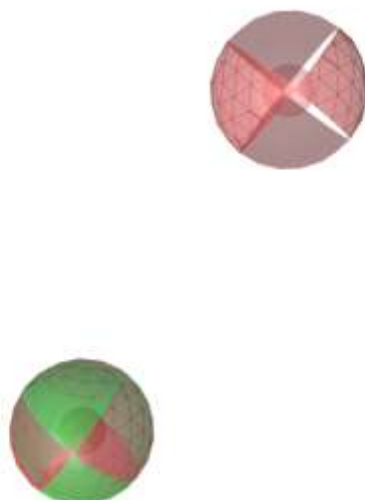
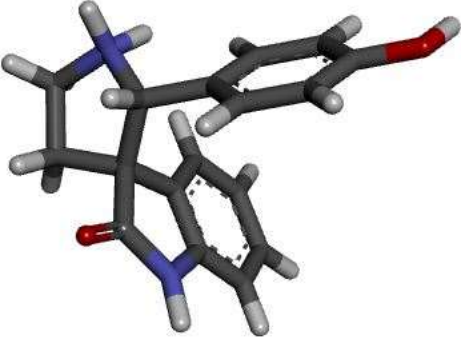
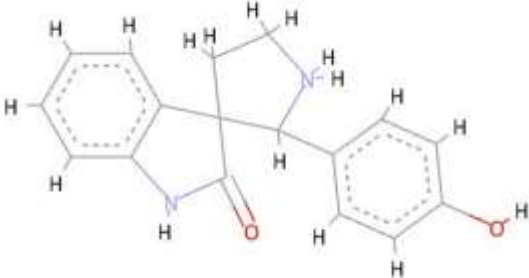
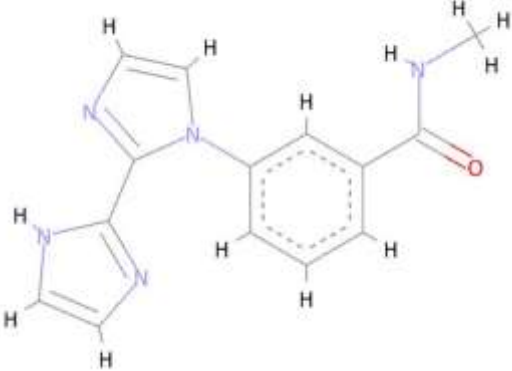


Figure 3.3: Consensus pharmacophore incorporating the critical pharmacophoric features of the optimal conformer of niclosamide and those of the crystallographically described ANP601 represented in PDB 5YJ9 (Okatsu *et al.*, 2018) rendered in LigandScout[®] (Wolber & Langer, 2005).

3.1.4 Affinity of the Molecules obtained through Virtual Screening for the Modelled PINK1 Protomol

The hits obtained from the online database ZINCPharmer[®] (Koes & Camacho, 2012) that were Lipinski rule complaint (Lipinski, 2011) were docked into the protomol and ranked in order of affinity (pK_d).

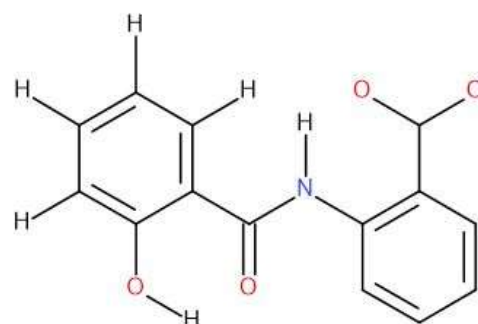
Table 3.1: A table showing the top six molecules obtained through virtual screening. Images rendered in Discovery Studio^{®1}.

Name	pK _d
ZINC40309676	6.56
	
ZINC72474970	6.48
	

²Biovia. Biovia Discovery Studio [Internet], United States of America; 2018 [cited 2020 Mar 16]. Available from: <http://accelrys.com/products/collaborative-science/biovia-discovery-studio/>

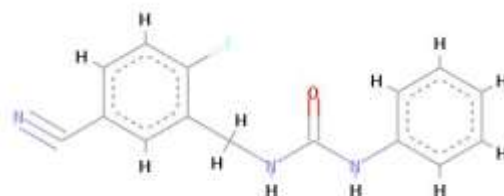
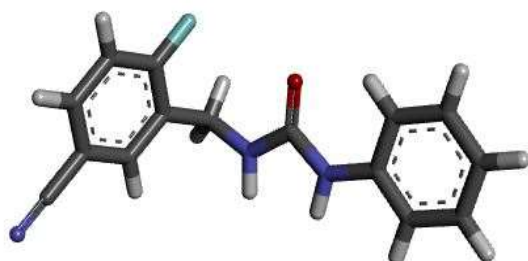
ZINC06567831

6.37



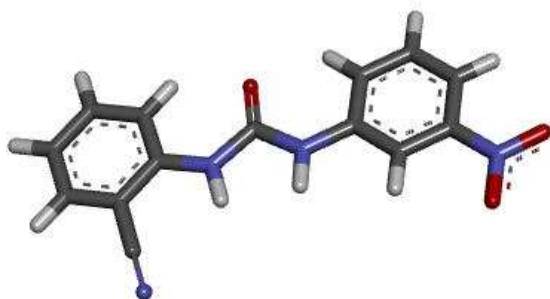
ZINC80617578

6.37



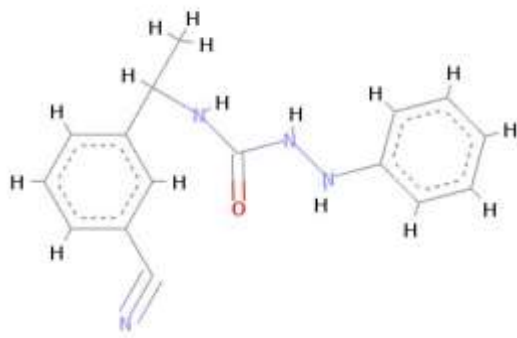
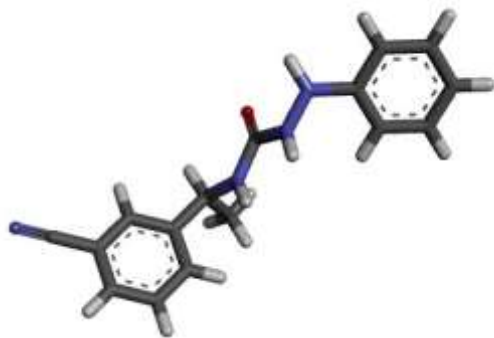
ZINC03851013

6.35



ZINC74918027

6.23

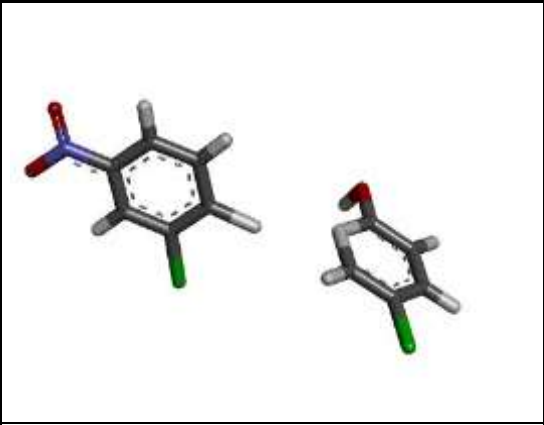
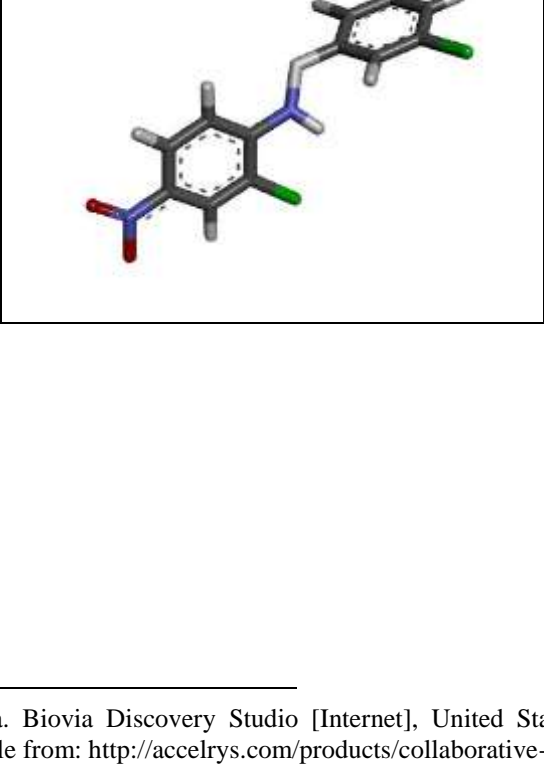
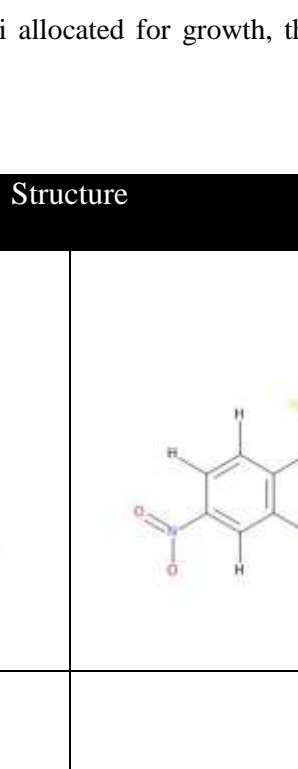
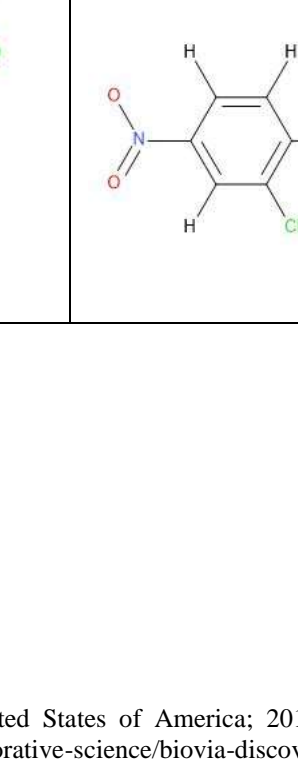


3.2 Results Obtained from *De Novo* Approach

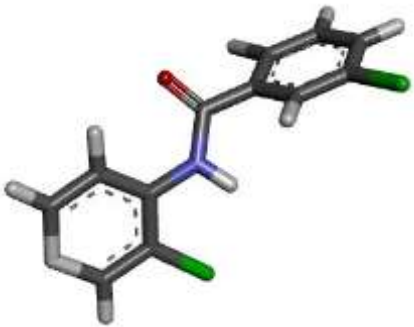
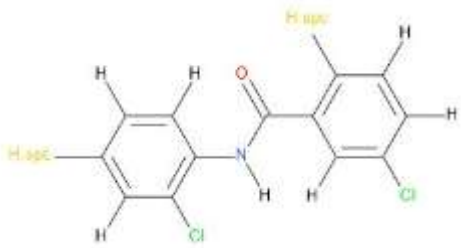
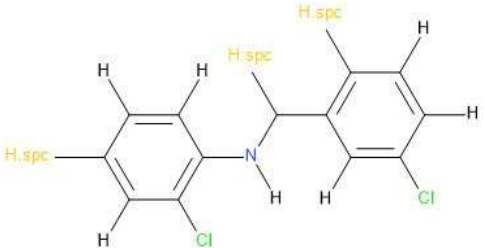
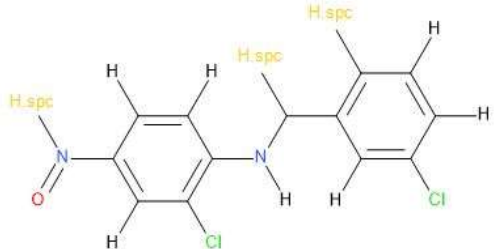
3.2.1 Seeds Generated from the Selected Optimal Conformer

Table 3.2: A table showing the five seed structures created from the de novo approach, along with the 2D structure indicating the exact loci allocated for growth, that is, the H.spc atom.

Images rendered in Discovery Studio^{®1}.

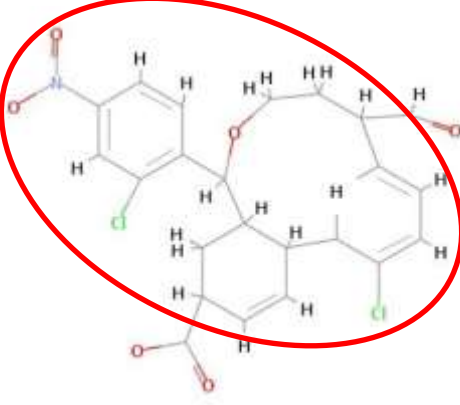
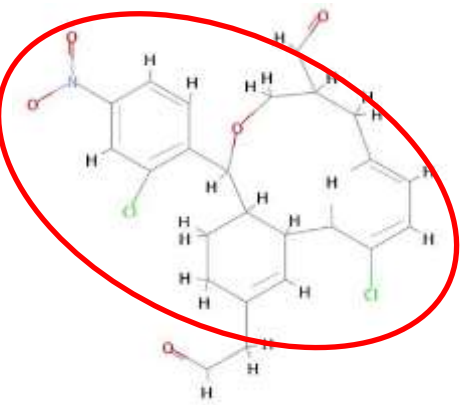
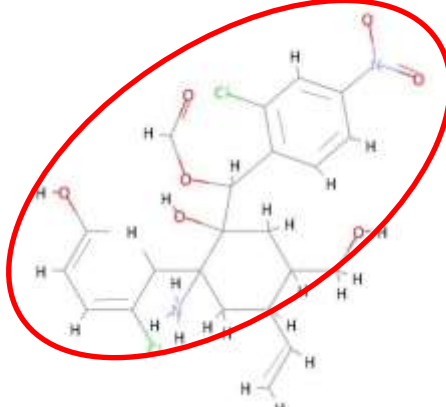
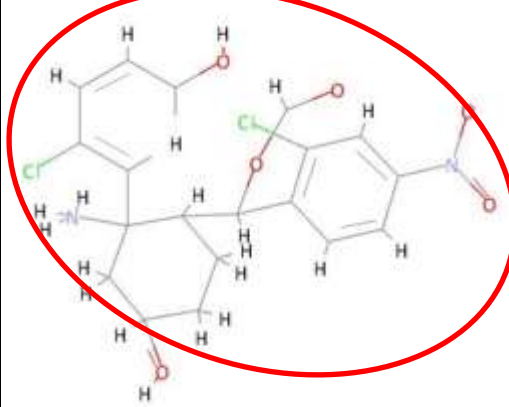
Seed	Structure	
1		
2		

¹ Biovia. Biovia Discovery Studio [Internet], United States of America; 2018 [cited 2021 Mar 16]. Available from: <http://accelrys.com/products/collaborative-science/biovia-discovery-studio/>

3		
4		
5		

3.2.2 Ligands Generated from the Seed Structures

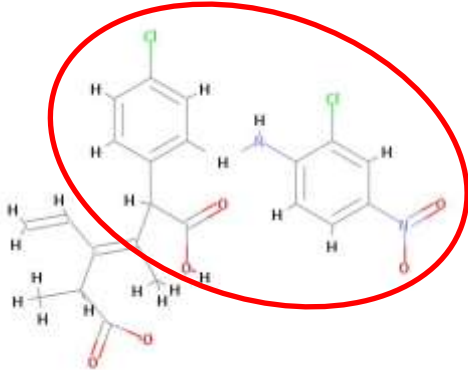
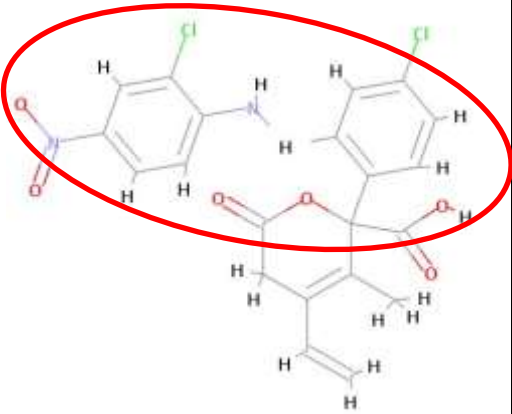
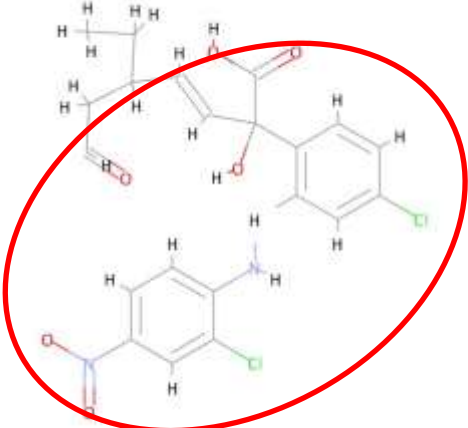
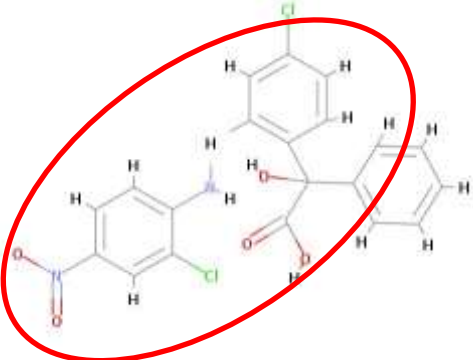
Table 3.3: A table comparing the structures of the ligands having the highest and lowest affinity towards the PINK1 receptor obtained from Seed 1. Images rendered in Discovery Studio^{®1}.

Family	Ligand with the highest affinity	Ligand with the lowest affinity
1	 $pK_d = 7.69$	 $pK_d = 6.47$
4	 $pK_d = 7.06$	 $pK_d = 6.02$

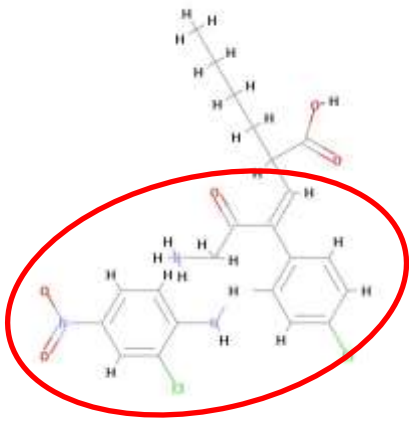
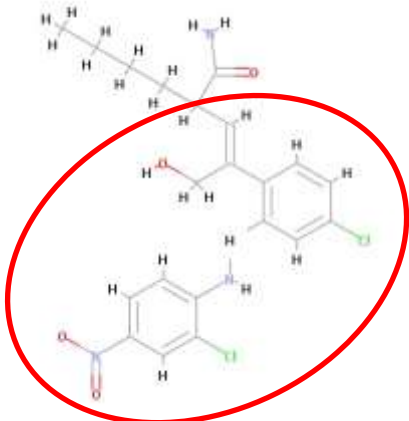
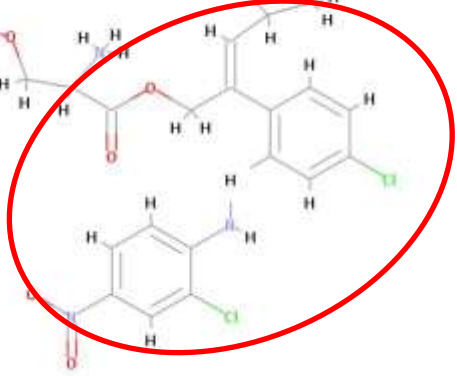
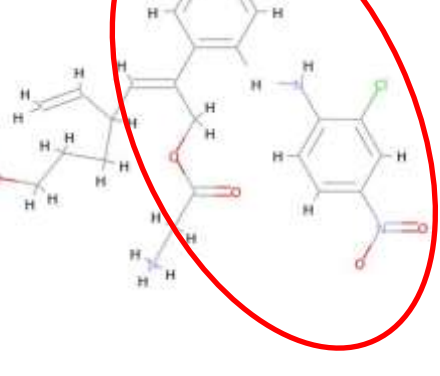
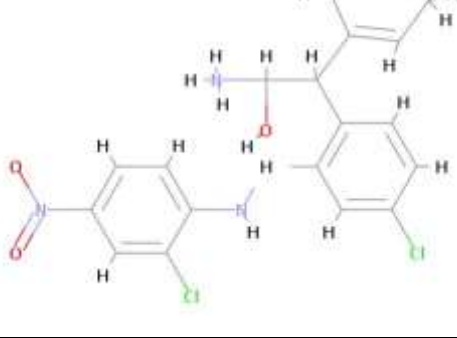
With reference to table 3.3, the carboxylic acid group has shown importance with regards to stability of the molecule and indicates a high affinity resulting from the ability of the carboxylic acid group to participate as both a HBA and HBD. The general pharmacophore of each family is indicated by the red circle.

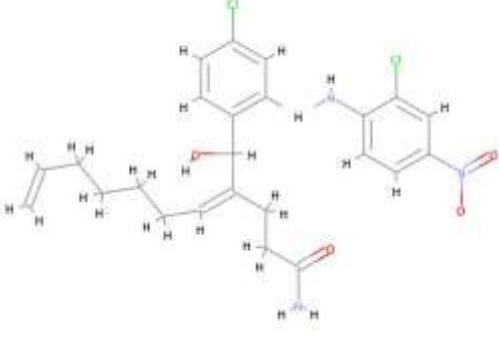
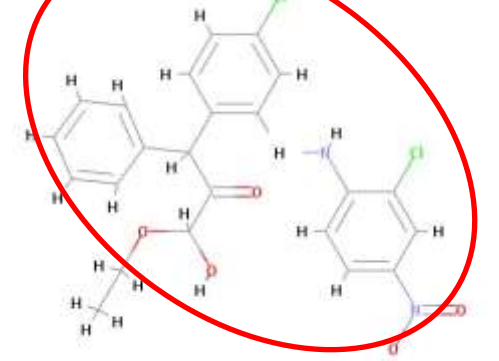
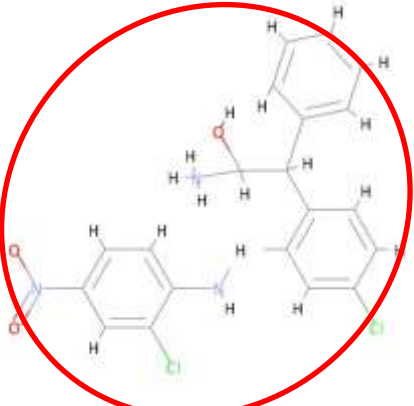
¹ Biovia. Biovia Discovery Studio [Internet], United States of America; 2018 [cited 2021 Mar 16]. Available from: <http://accelrys.com/products/collaborative-science/biovia-discovery-studio/>

Table 3.4: A table comparing the structures of the ligands having the highest and lowest affinity towards the PINK1 receptor obtained from Seed 2. Images rendered in Discovery Studio^{®1}.

Family	Ligand with the highest affinity	Ligand with the lowest affinity
1	 <p>$pK_d = 8.98$</p>	 <p>$pK_d = 8.78$</p>
2	 <p>$pK_d = 9.07$</p>	 <p>$pK_d = 8.72$</p>

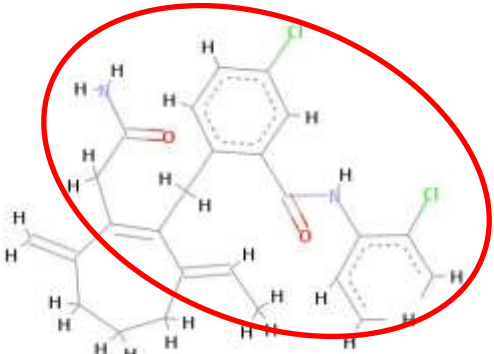
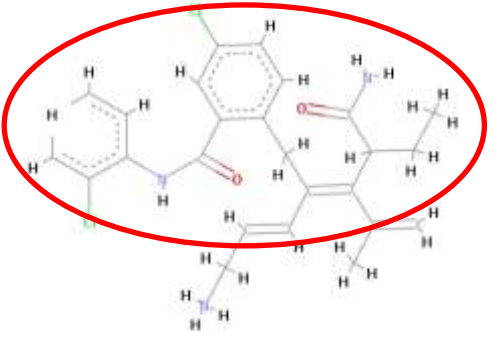
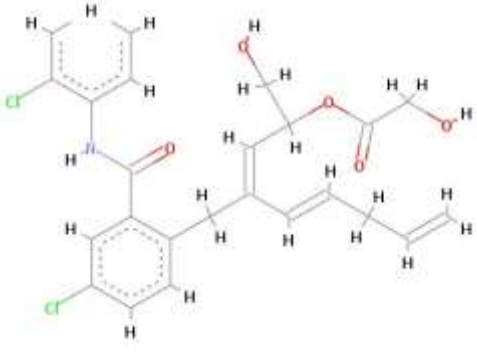
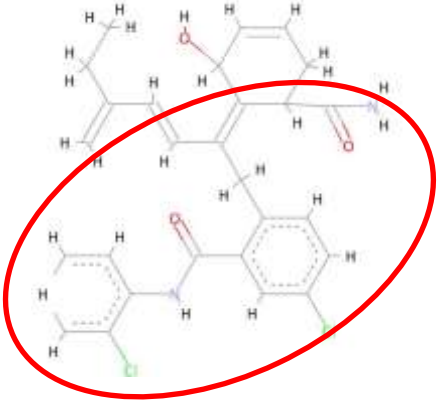
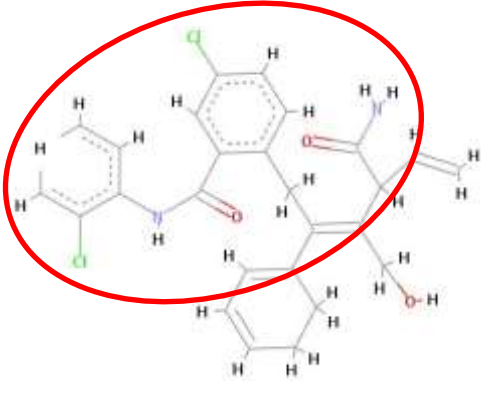
¹ Biovia. Biovia Discovery Studio [Internet], United States of America; 2018 [cited 2021 Mar 16]. Available from: <http://accelrys.com/products/collaborative-science/biovia-discovery-studio/>

4		
	$pK_d = 9.07$	$pK_d = 8.80$
5		
	$pK_d = 9.42$	$pK_d = 8.92$
8		N/A
	$pK_d = 9.13$	

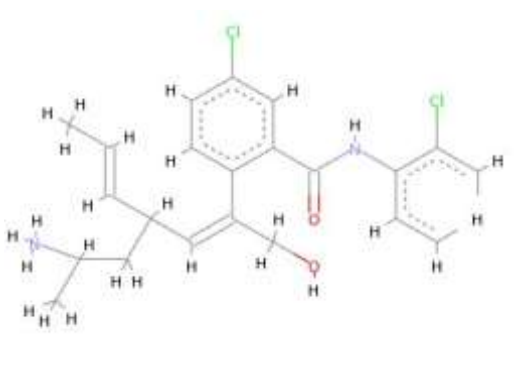
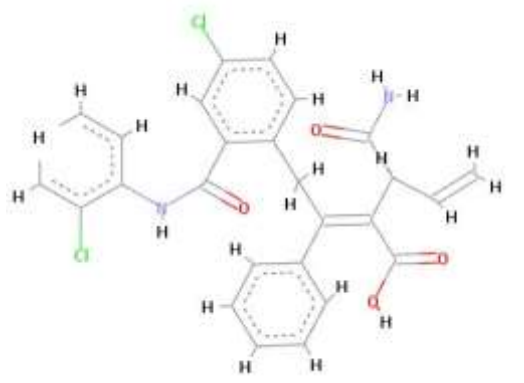
<p>10</p>		<p>N/A</p>
	<p>$pK_d = 8.81$</p>	
<p>11</p>		
	<p>$pK_d = 9.15$</p>	<p>$pK_d = 8.85$</p>

With reference to table 3.4, the carboxylic acid group, similar to seed 1, has shown an increase in affinity. The molecules with the highest affinity towards the PINK1 LBP, specifically those in family 5 and 11, are esters that participate as HBA. The general pharmacophore of each family is indicated by the red circle.

Table 3.5: A table comparing the structures of the ligands having the highest and lowest affinity towards the PINK1 receptor obtained from Seed 3. Images rendered in Discovery Studio^{®1}.

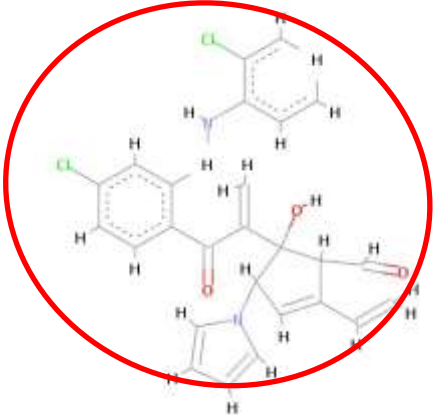
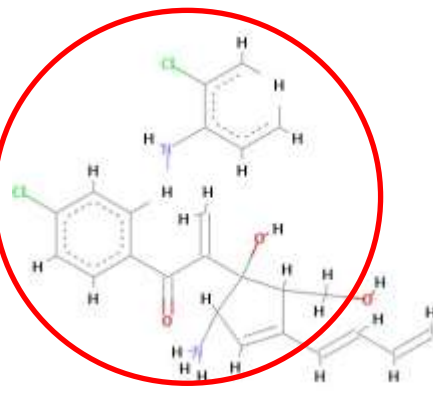
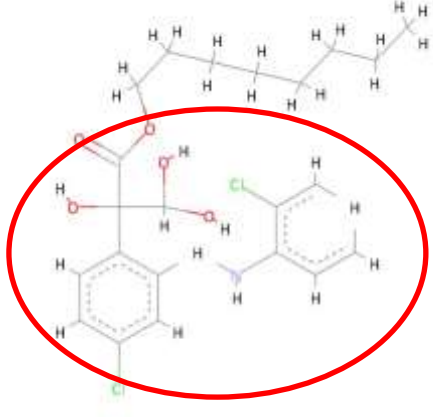
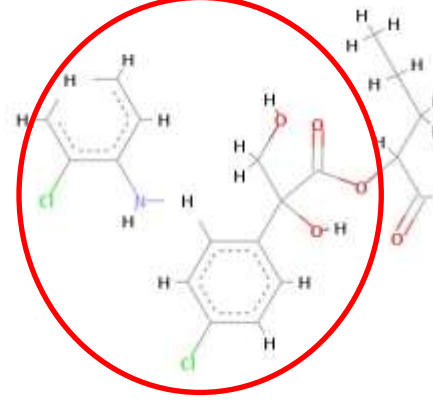
Family	Ligand with the highest affinity	Ligand with the lowest affinity
1	 <p>$pK_d = 8.80$</p>	 <p>$pK_d = 8.45$</p>
4	 <p>$pK_d = 8.63$</p>	N/A
5	 <p>$pK_d = 8.71$</p>	 <p>$pK_d = 8.66$</p>

¹ Biovia. Biovia Discovery Studio [Internet], United States of America; 2018 [cited 2021 Mar 16]. Available from: <http://accelrys.com/products/collaborative-science/biovia-discovery-studio/>

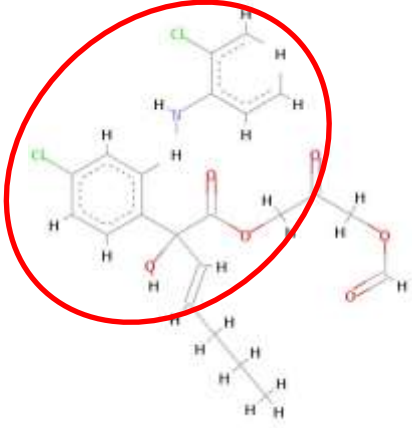
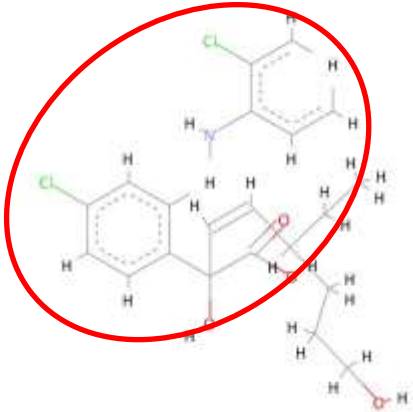
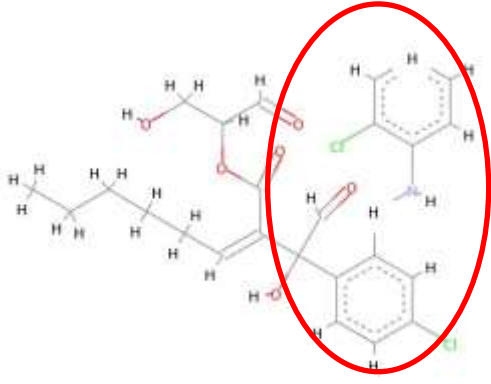
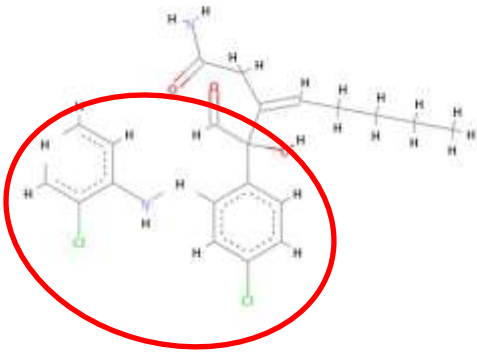
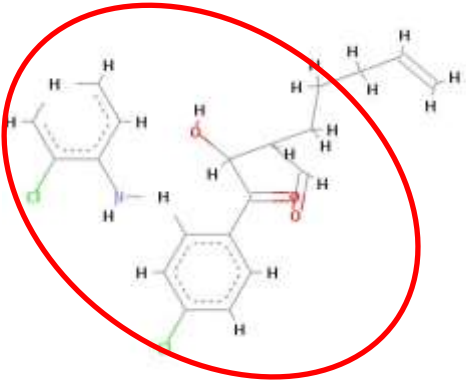
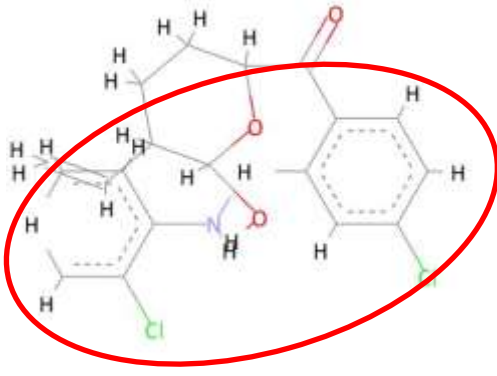
6		N/A
$pK_d = 8.47$		
7		N/A
$pK_d = 8.81$		

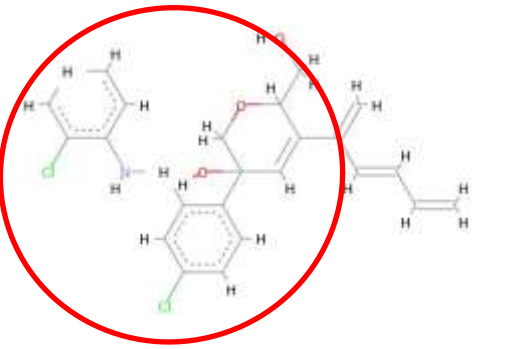
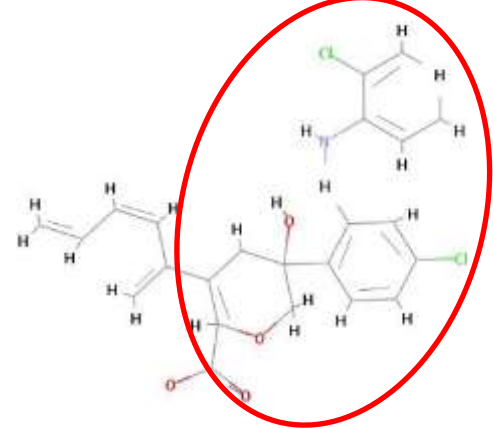
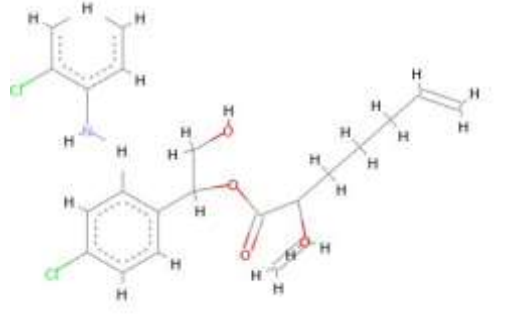
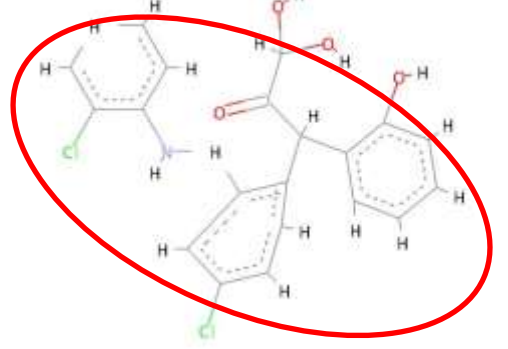
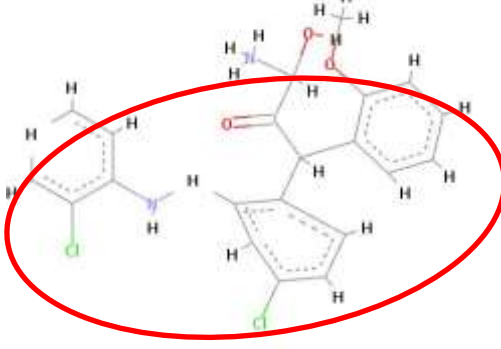
Structures having more carbon to carbon double bonds are shown to have a higher affinity towards the PINK1 LBP, which can be seen in table 3.5. The general pharmacophore of each family is indicated by the red circle.

Table 3.6: A table comparing the structures of the ligands having the highest and lowest affinity towards the PINK1 receptor obtained from Seed 4. Images rendered in Discovery Studio^{®1}.

Family	Ligand with the highest affinity	Ligand with the lowest affinity
1	 <p data-bbox="571 869 715 902">$pK_d = 8.61$</p>	 <p data-bbox="1102 869 1246 902">$pK_d = 8.39$</p>
2	 <p data-bbox="571 1384 715 1417">$pK_d = 9.95$</p>	 <p data-bbox="1102 1384 1246 1417">$pK_d = 8.49$</p>

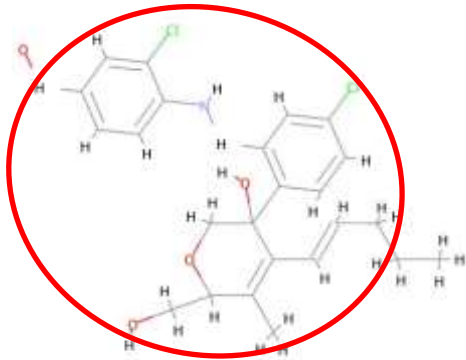
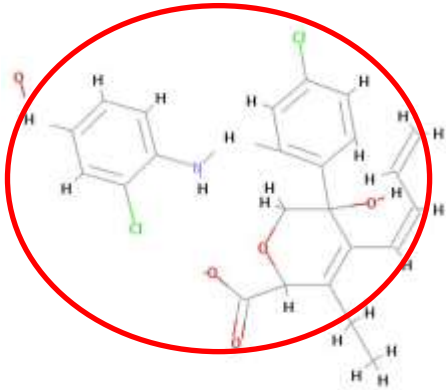
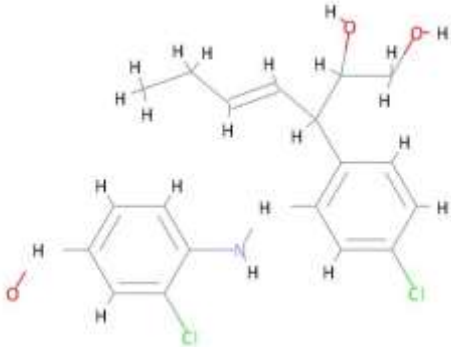
¹ Biovia. Biovia Discovery Studio [Internet], United States of America; 2018 [cited 2021 Mar 16]. Available from: <http://accelrys.com/products/collaborative-science/biovia-discovery-studio/>

4		
	$pK_d = 8.73$	$pK_d = 8.17$
5		
	$pK_d = 8.54$	$pK_d = 8.19$
6		
	$pK_d = 8.92$	$pK_d = 8.26$

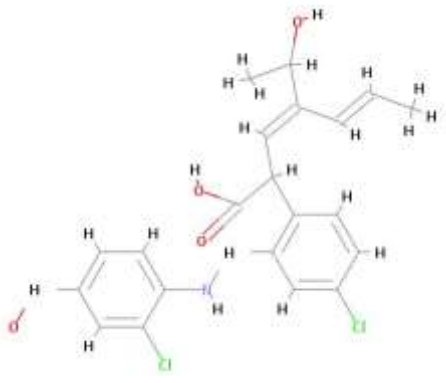
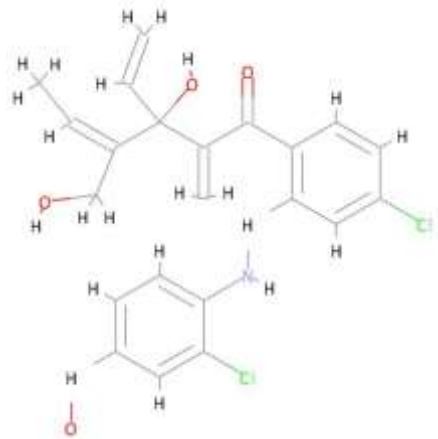
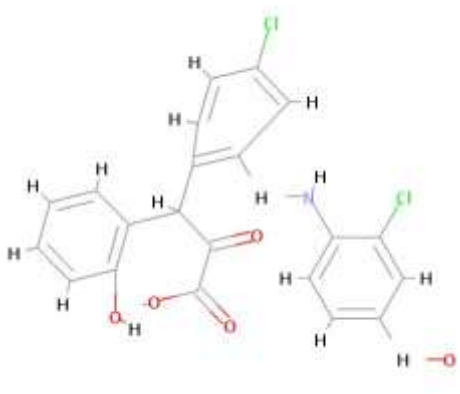
8		
	$pK_d = 9.12$	$pK_d = 8.16$
13		N/A
	$pK_d = 8.59$	
14		
	$pK_d = 8.43$	$pK_d = 8.26$

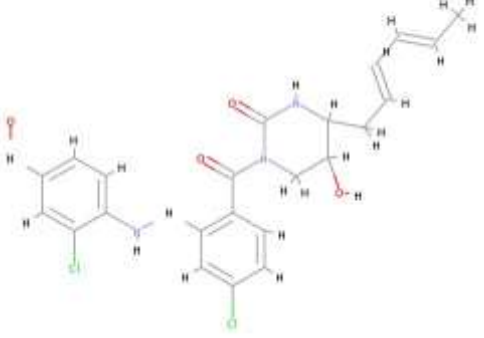
The molecules obtained from seed 4 had the highest affinity towards the PINK1 LBP, as can be observed in table 3.6. These molecules are esters, confirming that this increases affinity. When observing family 2 specifically, a long carbon chain is also attached to the ester moiety, whereas in the molecule having a lower affinity, a hydroxyl group is attached. For this reason, a hydroxyl group may decrease the affinity. The general pharmacophore of each family is indicated by the red circle.

Table 3.7: A table comparing the structures of the ligands having the highest and lowest affinity towards the PINK1 receptor obtained from Seed 5. Images rendered in Discovery Studio^{®1}.

Family	Ligand with the highest affinity	Ligand with the lowest affinity
3	 <p>$pK_d = 8.97$</p>	 <p>$pK_d = 8.38$</p>
7	 <p>$pK_d = 8.68$</p>	N/A

¹ Biovia. Biovia Discovery Studio [Internet], United States of America; 2018 [cited 2021 Mar 16]. Available from: <http://accelrys.com/products/collaborative-science/biovia-discovery-studio/>

<p>10</p>		<p>N/A</p>
<p>$pK_d = 8.87$</p>		
<p>11</p>		<p>N/A</p>
<p>$pK_d = 8.64$</p>		
<p>13</p>		<p>N/A</p>
<p>$pK_d = 8.42$</p>		

<p>15</p>		<p>N/A</p>
	<p>$pK_d = 8.42$</p>	

Through comparison of the moieties attached to the pharmacophore of family 3, observed in table 3.7, an alcohol group in this case has increased the affinity when it is accompanied by short carbon chains. The general pharmacophore of each family is indicated by the red circle.

Chapter 4:

Discussion

4. Discussion

Literature shows that PINK1 mutation drives early onset Parkinson's disease. There is also evidence that the anthelmintic drug niclosamide, and other molecules bearing its basic scaffold, activate PINK1 through reversible mitochondrial membrane potential impairment, resulting in slower disease development. The fact that niclosamide is a tried and tested molecule of good oral bioavailability and low toxicity, makes this scaffold very interesting from a repurposing perspective (Barini *et al.*, 2018). Therefore this project targeted the PINK1 receptor and used the niclosamide scaffold as a lead molecule for the *in silico* identification and design of high affinity PINK1 modulators, by adopting a dual approach.

Ligand-based VS, which was the first approach utilized, identified molecules based on the energetically unstable binding sites and the generated consensus pharmacophore. The results obtained vary drastically from a structural point of view when compared to niclosamide as molecules generated had no structural restrictions. This approach was therefore valuable because it allowed for innovation. The identified hit structures were allowed to be structurally diverse and were considered acceptable for further evaluation as long as they contained the pharmacophoric features described in the consensus pharmacophore, and as long as they were lead-like in nature.

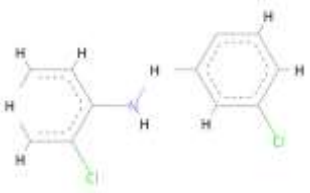
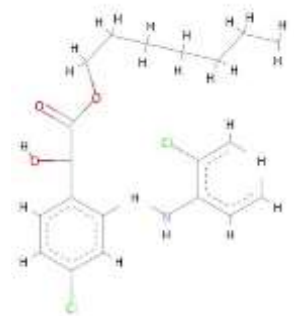
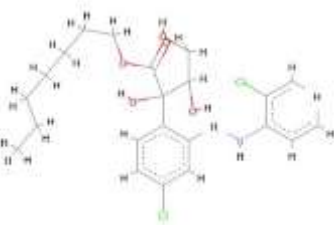
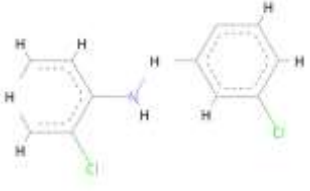
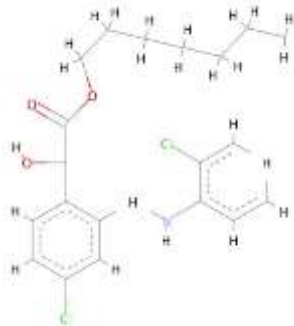
The second approach used was a structure-based technique, also known as the *de novo* approach that utilised a topology map of the critical interactions between the optimal niclosamide conformer and the PINK1 LBP to create high efficiency seed fragments. The structure of these fragments was therefore user driven, and contained, to different extents, the moieties considered critical to binding. These seed fragments were docked into the bioactive LBP and allowed to grow. The novel structures produced

were Lipinski rule compliant, and segregated into pharmacologically similar families for each seed fragment and ranked in order of affinity. The moieties preserved in the seed structures were consequently also preserved in all of the *de novo* generated ligands. This structural restriction in the *de novo* designed structures is in contrast with the structural diversity that was allowed in VS.

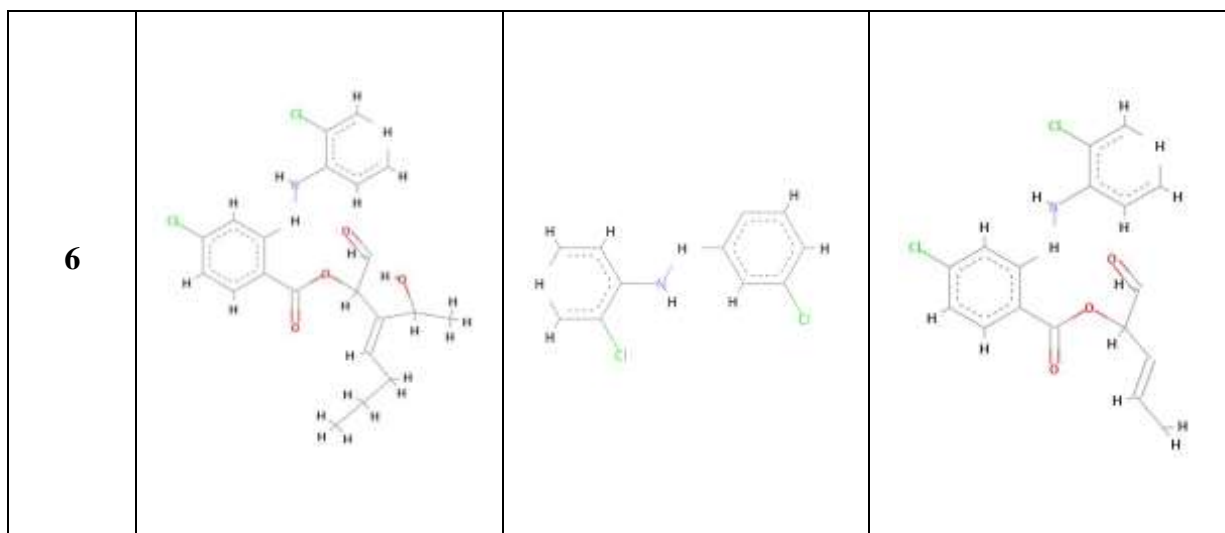
The method in which the *de novo* design process was carried out allowed for the recognition of two distinct pharmacophores. Reference is made to table 4.1. The first pharmacophore, P1, is the seed structure that was necessarily preserved in all daughter molecules. The second, P2, incorporated P1, but contained additional moieties that were the result of *de novo* growth. P2 was the unifying structural moiety present within each molecular family for each seed structure as categorised by the PROCESS module of LigBuilder[®] (Wang *et al.*, 2000).

As reported in section 3.2.2 of the results, the 3 optimal *de novo* structures all derived from seed 4 (table 3.4 on page 41). The pharmacophoric features of these molecules (P1 and P2) together with the structures of the 3 optimal derived molecules are shown in Table 4.1 below.

Table 4.1: 2D representations of the 3 optimal de novo designed molecules together with their respective pharmacophores P1 and P2. P1 is the user designed seed structure. Images rendered in Discovery Studio^{®1}.

Family	Molecular Structure	Pharmacophore 1	Pharmacophore 2
2			
2			

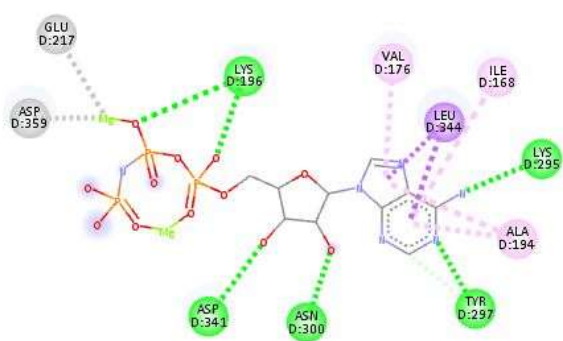
¹ Biovia. Biovia Discovery Studio [Internet], United States of America; 2018 [cited 2021 Mar 16]. Available from: <http://accelrys.com/products/collaborative-science/biovia-discovery-studio/>



The interactions forged between the optimal niclosamide conformer and the bioactive molecule ANP601 individually with the PINK1 LBP were analysed and the following similarities were noted;

- A hydrogen bond is forged between Lys¹⁹⁶ and the ligand
- A hydrophobic region is essential for the binding of the ligand with Ala¹⁹⁴ and Leu³⁴⁴
- A bond to Tyr²⁹⁷

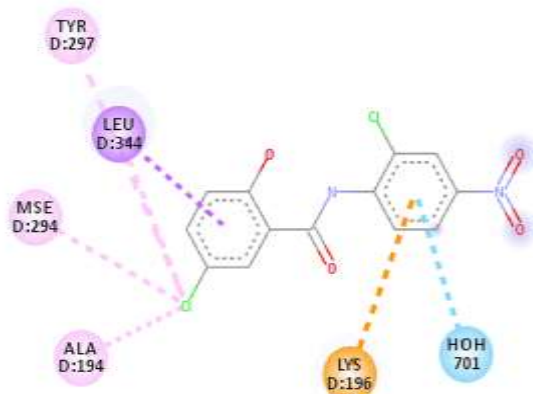
i.



Interactions

	Conventional Hydrogen Bond		Pi-Sigma
	Carbon Hydrogen Bond		Pi-Alkyl
	Metal-Acceptor		

ii.



Interactions

	Water Hydrogen Bond		Alkyl
	Pi-Cation		Pi-Alkyl
	Pi-Sigma		

Figure 4.1: Critical interactions forged between ANP601 (i) and the optimal niclosamide conformer (ii) to the PINK1 LBP. Images rendered in Discovery Studio^{®1}.

The interactions between the optimal niclosamide conformer and the 3 optimal structures obtained from the *de novo* approach were compared. This resulted in identification of the following binding similarities between the optimal niclosamide conformer and the *de novo* designed structures with the highest affinity for the PINK1 receptor.

¹ Biovia. Biovia Discovery Studio [Internet], United States of America; 2018 [cited 2021 Mar 16]. Available from: <http://accelrys.com/products/collaborative-science/biovia-discovery-studio/>

- A hydrophobic region is required for the interactions between the amino acids, Tyr²⁹⁷ and Ala¹⁹⁴ and the ligand, specifically the hydrophobic region was identified to be the chlorine of the chlorophenolate ring
- A pi-sigma bond is forged between Leu³⁴⁴ and the chlorophenolate ring

The interactions between the molecules having the highest affinity towards the PINK1 receptor were also compared which identified two hydrogen bonds formed between the alcohol and carbonyl groups of the molecule with Asp³⁴¹ and Asp³⁰⁰, thus indicating the importance relating to the affinity of these interactions.

This study resulted in two molecular cohorts, one identified through VS, and the other through *de novo* design, both of which were lead-like or Lipinski Rule compliant. The 3 optimal structures from an affinity perspective were identified in each case. The different cohorts emanating from distinct approaches had their respective merits and disadvantages. The molecules identified through VS had their affinity calculated for a modelled protomol, which, while representing the energetically unsatisfied space at the interior of the PINK1 receptor in its entirety had less potential to bioactivity than their *de novo* designed counterparts which were built into a pharmacophoric space described through X-ray crystallography as being bioactive. This means, on the other hand, that while the *de novo* designed structures were structurally more restricted, they had a higher bioactive potential.

The implication therefore is that the optimal structures obtained through each applied approach must be validated separately. There must be more rigorous investigation of the bioactivity of the molecules obtained through VS.

The *de novo* designed molecules are more structurally related to the lead molecule niclosamide whose scaffold was proposed for repurposing in this study. The fact that

the *de novo* designed structures are designed from niclosamide, does not guarantee similar bioavailability and toxicity profiles. Indeed, these should be addressed in later stages of their optimisation. However, this study has been instrumental in showing that niclosamide does indeed bind to the PINK1 receptor, with an affinity (5.36) albeit lower than those of its *de novo* designed counterparts. The implication is that niclosamide, about which there is a wealth of pharmacokinetic information available, should continue to be given consideration in its own right.

The major shortcoming of this study is the fact that at no time were dynamic studies attempted. Molecular dynamic studies are important validation tools, and should be utilised in the first optimisation round of the optimal structures identified in this study as the first predictors of their bioactivity.

References

Ash S, Cline M, Homer R, Hurst T, Smith GB. Sybyl Line Notation (SLN): A versatile Language for Chemical Structure Representation. *J Chem Inf Comput Sci.* 1997; 37(1):71-79.

Barini E, Miccoli A, Tinarelli F, Mulholland K, Kadri H, Khanim F, *et al.* The Anthelmintic Drug Niclosamide and Its Analogues Activate the Parkinson's Disease Associated Protein Kinase PINK-1. *ChemBioChem.* 2018; 19(5):425-429.

Beilina A, Van Der Brug M, Ahmad R, Kesavapany S, Miller D, Petsko G, *et al.* Mutations in PTEN-induced putative kinase 1 associated with recessive parkinsonism have differential effects on protein stability. *Proc Natl Acad Sci U S A.* 2005; 102 (16): 5703-5708.

Chaudhuri K, Clough C, Sethi K. *Fast Facts Parkinson's Disease.* Abingdon: Health Press Ltd.; 2011.

Congreve M, Carr R, Murray C, Jhoti H. A 'Rule of Three' for fragment-based lead discovery?. *Drug Discov Today.* 2003; 8(19):876-877.

Daou S, Sicheri F. Vivid views of the PINK-1 protein. *Nature.* 2017; 552(7683):38-39.

Darong K, So-Yeon K, Dongyoung K, Nam Gu Y, Jisu Y, Ki Bum H, *et al.* Development of pyrazolo[3,4-*d*]pyrimidine-6-amine-based TRAP1 inhibitors that demonstrate *in vivo* anticancer activity in mouse xenograft models. *Bioorg Chem.* 2020; 101: 103901.

Galati S, Di Giovanni G. Neuroprotection in Parkinson's Disease: a Realistic Goal? *CNS Neurosci Ther.* 2010; 16(6):327-329.

Gies E, Wilde I, Winget J, Brack M, Rotblat B, Novoa C, et al. Niclosamide prevents the formation of large ubiquitin-containing aggregates caused by proteasome inhibition. PLoS One [Internet]. 2010 [cited 2021 Mar 16]; 5(12): e14410. Available from: <https://doi.org/10.1371/journal.pone.0014410>

Hilbig M, Rarey M. MONA 2: a light cheminformatics platform for interactive compound library processing. J Chem Inf Model. 2015; 55(10):2071–2078.

Kadri H, Lambourne O, Mehellou Y. Niclosamide, a Drug with Many (Re)purposes. ChemMedChem. 2018; 13(11):1088-1091.

Koes D, Camacho C. ZINCPharmer: pharmacophore search of the ZINC database. Nucleic Acids Res. 2012; 40(W1):W409-W414.

Lambourne O, Mehellou Y. Chemical Strategies for Activating PINK-1, a Protein Kinase Mutated in Parkinson's Disease. ChemBioChem. 2018; 19(23):2433-2437.

Lazarou M, Sliter D, Kane L, Sarraf S, Wang C, Burman J, et al. The ubiquitin kinase PINK-1 recruits autophagy receptors to induce mitophagy. Nature. 2015; 524(7565):309-314.

Leites E, Morais V. Mitochondrial quality control pathways: PINK1 acts as a gatekeeper. Biochem Biophys Res Commun. 2018; 500(1):45-50.

Li W, Srinivasula S, Chai J, Li P, Wu J, Zhang Z, et al. Structural insights into the proapoptotic function of mitochondrial serine protease HtrA2/Omi. Nat Struct Biol. 2002; 9(6):436-441.

Lipinski C. Drug repurposing. *Drug Discov Today Ther Strateg.* [Internet] 2011 [cited 2021 Mar 16]; 8(3-4):57-59. Available from: https://www.researchgate.net/publication/257687350_Drug_repurposing

Lu L, Jia H, Gao G, Duan C, Ren J, Li Y, *et al.* PINK1 Regulates Tyrosine Hydroxylase Expression and Dopamine Synthesis. *J Alzheimers Dis.* 2018; 63(4):1361-1371.

Mandal S, Moudgil M, Mandal S. Rational drug design. *Eur J Pharmacol.* 2009; 625(1-3):90-100.

Manion M, O'Neill J, Giedt C, Kim K, Zhang K, Hockenbery D. Bcl-XL Mutations Suppress Cellular Sensitivity to Antimycin A. *J Biol Chem.* 2004; 279(3):2159-2165.

Okatsu K, Sato Y, Yamano K, Matsuda N, Negishi L, Takahashi A, *et al.* Structural insights into ubiquitin phosphorylation by PINK1. *Sci Rep.* [Internet] 2018 [cited 2021 Mar 21]; 8(1). Available from: <https://doi.org/10.1038/s41598-018-28656-8>

Oprea T, Mestres J. Drug Repurposing: Far Beyond New Targets for Old Drugs. *AAPS J* [Internet]. 2012 [cited 2021 Mar 16]; 14(4):759-763. Available from: <https://www.ncbi.nlm.nih.gov/pubmed/22826034>

Pantziarka P, Bouche G, Meheus L, Sukhatme V, Sukhatme V, Vikas P. the Repurposing Drugs in Oncology (ReDO) Project. *Ecancermedicalsecience.* [Internet] 2014 [cited 2021 Mar 16]; 8: 422. Available from: <https://ecancer.org/en/journal/article/442-the-repurposing-drugs-in-oncology-redo-project>

Parenti M, Rastelli G. Advances and applications of binding affinity prediction methods in drug discovery. *Biotechnol Adv.* 2012; 30(1): 244-250.

Petterson EF, Goddard TD, Huang CC, Couch GS, Greenblatt DM, Meng EC, et al. UCSF Chimera—a visualization system for exploratory research and analysis. *J Comput Chem.* 2004;25(13):1605-12.

Pickrell A, Youle R. The roles of PINK1, parkin, and mitochondrial fidelity in Parkinson's disease. *Neuron.* 2015; 85(2): 257-273.

Pinto C. An industry update: what is the latest news in the therapeutic delivery field? *Ther Deliv.* 2018; 9(5).

Plun-Favreau H, Klupsch K, Moiso N, Gandhi S, Kjaer S, Frith D, *et al.* The mitochondrial protease HtrA2 is regulated by Parkinson's disease-associated kinase PINK1. *Nat Cell Bio.* 2007; 9(11): 1243- 1252.

Poewe W, Seppi K, Tanner C, Halliday G, Brundin P, Volkman J, *et al.* Parkinson disease. *Nat Rev Dis Primers.* [Internet] 2017 [cited 2021 Mar 16]; 3: 17013. Available from: <https://www.ncbi.nlm.nih.gov/pubmed/28332488>

Radhakrishnan D, Goyal V. Parkinson's disease: A review. *Neurol India.* 2018; 66(7):26-35.

Reddy M. Editorial [Hot Topic: Rational Drug Design (Executive Editor: M. Rami Reddy)]. *Curr Pharm Des.* 2007; 13(34):3453-3453.

Riley B, Loughheed J, Callaway K, Velasquez M, Brecht E, Nguyen L, *et al.* Structure and function of Parkin E3 ubiquitin ligase reveals aspects of RING and HECT ligases. *Nat Commun.* [Internet] 2013 [cited 2021 Mar 16]; 4(1): 1982. Available from: <https://www.ncbi.nlm.nih.gov/pubmed/23770887>

Shan Y, Liu B, Li L, Chang N, Li L, Wang H, *et al.* Regulation of PINK-1 by NR2B-containing NMDA receptors in ischemic neuronal injury. *J Neurochem.* 2009; 111(5):1149-1160.

Song S, Jang S, Park J, Bang S, Choi S, Kwon K, *et al.* Characterization of PINK-1 (PTEN-induced Putative Kinase 1) Mutations Associated with Parkinson Disease in Mammalian Cells and *Drosophila*. *J Biol Chem.* 2013; 288(8):5660-5672.

Strauss K, Martins L, Plun-Favreau H, Marx F, Kautzmann S, Berg D, *et al.* Loss of function mutations in the gene encoding Omi/HtrA2 in Parkinson's disease. *Hum Mol Genet.* 2005; 14(15): 2099-2111.

Strittmatter S. Overcoming Drug Development Bottlenecks With Repurposing: Old drugs learn new tricks. *Nat Med.* 2014; 20(6):590-591.

Triplett J, Zhang Z, Sultana R, Cai J, Klein J, Büeler H, *et al.* Quantitative expression proteomics and phosphoproteomics profile of brain from PINK-1 knockout mice: insights into mechanisms of familial Parkinson's disease. *J Neurochem.* 2015; 133(5):750-765.

Veber D, Johnson S, Cheng H, Smith B, Ward K, Kopple K. Molecular properties that influence the oral bioavailability of drug candidates. *J Med Chem.* 2002; 45(12): 2615-2623.

Vincow E, Merrihew G, Thomas R, Shulman N, Beyer R, MacCoss M, *et al.* The PINK-1-Parkin pathway promotes both mitophagy and selective respiratory chain turnover in vivo. *Proc Natl Acad Sci U S A.* 2013; 110(16):6400-6405.

von Stockum S, Marchesan E, Ziviani E. Mitochondrial quality control beyond PINK-1/Parkin. *Oncotarget*. [Internet] 2018 [cited 2021 Mar 16]; 9(16): 12550-12551. Available from: <https://pubmed.ncbi.nlm.nih.gov/29560088/>

Walden H, Podgorski M, Huang D, Miller D, Howard R, Minor D, *et al*. The Structure of the APPBP1-UBA3-NEDD8-ATP Complex Reveals the Basis for Selective Ubiquitin-like Protein Activation by an E1. *Mol Cell*. 2003; 12(6):1427-1437.

Wang R, Gao Y, Lai L. LigBuilder: A multi-purpose program for structure-based drug design. *J Mol Model*. 2000; 6: 498-516.

Wang R, Lai L, Wang S. Further development and validation of empirical scoring functions for structure-based binding affinity prediction. *J Comput Aided Mol Des*. 2002; 16(1): 11-26.

Wolber G, Langer T. LigandScout: 3-D pharmacophores derived from protein-bound ligands and their use as virtual screening filters. *J Chem Inf Model*. 2005; 45(1):160-169.

Ye T, Xiong Y, Yan Y, Xia Y, Song X, Liu L, *et al*. The anthelmintic drug niclosamide induces apoptosis, impairs metastasis and reduces immunosuppressive cells in breast cancer model. *PLoS One* [Internet]. 2014 [cited 2021 Mar 16]; 9(1): e85887. Available from: <https://journals.plos.org/plosone/article?id=10.1371/journal.pone.0085887>

Zhi L, Qin Q, Muqem T, Seifert E, Liu W, Zheng S, *et al*. Loss of PINK1 causes age-dependent decrease of dopamine release and mitochondrial dysfunction. *Neurobiol Aging*. 2019; 75:1-10.

List of Publications and Abstracts

Abstract submitted to Current Neuropharmacology.

Abstract for the proposed Article:

(Please copy and paste the Abstract in the space provided below. You may also type it directly. The abstract should not exceed 250 words and it should condense the essential features of the review article, with the focus on the major advances in the field.)

*Title of the proposed Article:

Validation of the Repurposing of the Niclosamide Scaffold for the Design of PTEN-induce

*Contributing Authors:

Abigail Buttigieg, Dr. Claire Shoemake

*Author Affiliations:

Department of Pharmacy, University of Malta

*Abstract:

A mutation in the PTEN-induced putative kinase 1 (PINK 1) receptor has been shown to drive early onset Parkinson's disease. Evidence suggests that the anthelmintic drug niclosamide, shown to have good oral bioavailability and low toxicity, and other molecules bearing its basic scaffold are capable of activating PINK 1 through reversible mitochondrial membrane potential impairment resulting in a slower disease development. Thus PINK 1 is a target for the design of novel anti-parkinsonian drugs. This project aims to use the niclosamide scaffold as a lead molecule for the *in silico* identification and design of high affinity PINK 1 modulators.

*Keywords:

Parkinson's Disease, Niclosamide, Drug Repurposing

*Tentative date for submission of complete manuscript:

1st October 2021

Appendix A: Ethics Approval

8/30/2021

Gmail - FRECMDS_2021_184 - ID:-9562_24082021_Abigail Buttigieg



Abigail Buttigieg <abigailbuttigieg@gmail.com>

FRECMDS_2021_184 - ID:-9562_24082021_Abigail Buttigieg

FACULTY RESEARCH ETHICS COMMITTEE <research-ethics.ms@um.edu.mt>

Mon, Aug 30, 2021 at 11:31 AM

To: Abigail Buttigieg <abigailbuttigieg@gmail.com>

Cc: Claire Shoemake <claire.zerafa@um.edu.mt>

Dear Ms Buttigieg,

Since your self-assessment resulted in no issues being identified, FREC will file your application for record and audit purposes but will not review it.

Any ethical and legal issues including data protection issues are your responsibility and that of the supervisor.

Good luck with your project!

Regards,

Annalise

[Quoted text hidden]

[Quoted text hidden]

Addendum

A CD containing all the relevant raw data used in this project includes;

- A file containing the LBA of all twenty conformers of niclosamide and ANP601
- A word document containing the LBE of all twenty conformers of niclosamide and ANP601
- An excel file containing all Lipinski rule complaint molecules generated from the VS approach
- An index file from all seeds of the *de novo* results
- An excel file containing all Lipinski rule complaint molecules generated from the *de novo* approach.